

Review

# Cesium Heteropolyacid Salts: Synthesis, Characterization and Activity of the Solid and Versatile Heterogeneous Catalysts

Marcio Jose da Silva <sup>\*</sup>, Alana Alves Rodrigues  and Neide Paloma Gonçalves Lopes

Chemistry Department, Federal University of Viçosa, Viçosa 36570-000, Minas Gerais, Brazil

<sup>\*</sup> Correspondence: silvamj2003@ufv.br

**Abstract:** Keggin-type heteropolyacid cesium salts have been regarded as potential candidates for heterogeneous catalytic reactions. This review describes the success of Keggin-type heteropolyacids cesium salts (Cs-HPA salts) as efficient catalysts in various synthesis processes. The Cs-HPA catalysts can be synthesized as solid salts through the metathesis of a solution containing precursor HPA and another solution containing soluble Cs salt, which will give Cs-HPA salt as a solid precipitate. Alternatively, they can be also obtained from the commercial precursor HPA. In this review, all the routes to prepare the different cesium salts (i.e., saturated, lacunar, metal-doped) were described. These salts can be used in acid-catalyzed reactions (i.e., esterification, etherification, acetalization, dehydration) or oxidative transformations (oxidative esterification, oxidation, epoxidation). All of these reactions were addressed herein. Aspects related to the synthesis and characterization of these catalyst salts were discussed. This review aims to discuss the most pertinent heterogeneous catalytic systems based on Keggin HPA Cs salts. The focus was to correlate the physicochemical properties of these salts with their catalytic activity. Ultimately, the most recent advances achieved in the applications of these Cs-HPA salts as catalysts in the synthesis of industrial interest compounds were discussed. Cesium heteropoly salts are an alternative to the traditional soluble mineral acids as well as to solid-supported catalysts.

**Keywords:** Keggin heteropolyacids; solid heterogenous catalysts; transition metal-doped cesium salts; lacunar cesium salts



**Citation:** da Silva, M.J.; Rodrigues, A.A.; Lopes, N.P.G. Cesium Heteropolyacid Salts: Synthesis, Characterization and Activity of the Solid and Versatile Heterogeneous Catalysts. *Chemistry* **2023**, *5*, 662–690. <https://doi.org/10.3390/chemistry5010047>

Academic Editors: José Antonio Odriozola and Hermenegildo García

Received: 3 February 2023

Revised: 7 March 2023

Accepted: 13 March 2023

Published: 21 March 2023



**Copyright:** © 2023 by the authors. Licensee MDPI, Basel, Switzerland. This article is an open access article distributed under the terms and conditions of the Creative Commons Attribution (CC BY) license (<https://creativecommons.org/licenses/by/4.0/>).

## 1. Introduction

The development of heterogeneous catalysts has attracted widespread attention due to economic and environmental reasons [1,2]. Important characteristics such as simple synthesis routes, uniform pore size distribution, large specific surface area, and high strength of acidity are essential to an efficient solid acid catalyst. Ideally, a heterogeneous catalyst should be stable under reaction conditions, operate for long periods without the necessity of activation steps, achieve high conversions and selectivity toward the goal product, and allow an easy recovery and reuse without loss activity [3,4]. Nonetheless, understanding the reaction mechanisms involved in the conversion of different substrates over heterogeneous catalysts to fine chemicals or fuels is still a challenge [5–7].

Zeolites, clays, molecular sieves, sulfonated carbon, sulfonic resins, nano-, meso-, or microstructures solids are the most common choices for acid-catalyzed reactions, however, sometimes some drawbacks hamper the use of these catalysts at the industrial scale [8–10]. The high cost of these heterogeneous catalysts besides the laborious syntheses and the requirements of more drastic reaction conditions comprises some challenges to be overcome [11].

Keggin heteropolyacids (HPAs) are acid solids with a high strength of Brønsted acidity [12]. They are a cluster of metal-oxygen compounds belonging to the class of polyoxometalate (POMs) and have been used in several fields in materials and catalysis science, such as energy store, photocatalyst, electrocatalysis, and as homogeneous or

heterogeneous catalysts [13–15]. Keggin HPAs are protonated POMs with a stronger acidity strength [16]. Among them, phosphotungstic acid deserves highlighting due to its highest Brønsted acidity strength [17,18]. However, they are solid with a low surface area ( $<5.0 \text{ m}^2/\text{g}$ ), hampering their straight use as a heterogeneous catalyst [19,20]. Moreover, they are soluble in water or polar organic solvents. However, even having a low surface area, in apolar solvents they are insoluble and can be used as solid catalysts, likewise the cesium salts.

To circumvent these drawbacks, two options have been adopted; the first one and the more traditional, which is to support the Keggin KPAs on the surface area high solids matrixes [21]. Depending on the synthesis processes, catalyst load and type of support, positive aspects have been achieved [22]. For instance, H $\beta$  zeolite, zirconium, niobium, silica, activated carbon, and mesoporous materials (i.e., SBA, MCM) have been the most common supports selected [23–28]. Notwithstanding, these supported catalysts have the same disadvantages as other ones mentioned herein, such as undergoing leaching in a highly polar reaction medium.

The strength of acidity of Keggin HPAs can be modulated by performing modifications either in the structure of Keggin heteropolyanion or changing total or partially their protons with other metal cations [29]. This way, Keggin HPAs containing both Lewis and Brønsted acid sites have been developed. Even when all the protons are exchanged with a metal cation, remains a residual Brønsted acidity.

On the other hand, Keggin HPAs can have their composition modified by removing one unit MO (M = W, Mo) giving origin to the lacunar HPAs, or still having this vacancy filled with transition metal cations [30]. Those POMs salts can also have their Mo<sup>6+</sup> or W<sup>6+</sup> addenda cations replaced by V<sup>5+</sup> ions [31]. All these modifications allow Keggin HPAs, initially used only in acid-catalyzed reactions, to become also efficient catalysts in oxidation processes [32,33].

The second approach is converting the Keggin HPAs to solid salts, which can be used as heterogeneous catalysts. Depending on the cation ionic radius, it is possible to produce materials with a reasonable surface area and porosity, and insoluble in polar solvents [34]. In particular, cesium-exchanged Keggin heteropolyacid salts have been the most used catalysts, and therefore, they are the goal of this work [35–37]. Although presently the supporting of Keggin Cs HPA salts on solid matrixes has also attracted attention, we judge it more profitable to address only the reactions where these salts were used as solid catalysts, avoiding this way the effects triggered by the support.

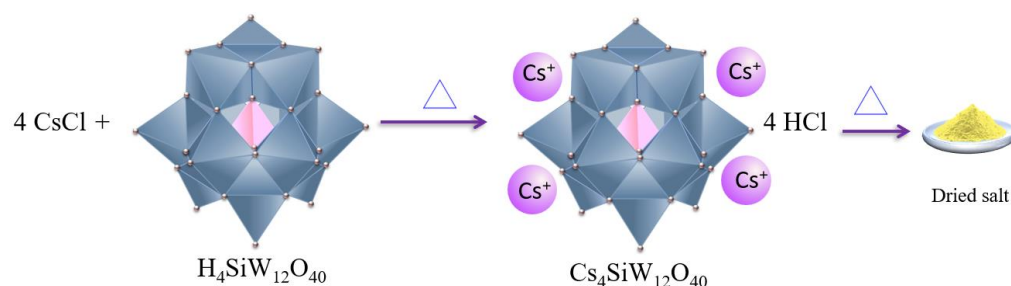
In this review, our main goal was to demonstrate how the Keggin HPAs Cs salts act as heterogeneous catalysts in a plethora of organic transformations. The main synthesis routes and characterization techniques will be discussed, aiming to correlate their impacts on the catalytic performance of these Keggin HPAs Cs salts.

## 2. Main Routes to Synthesize POMs Salts

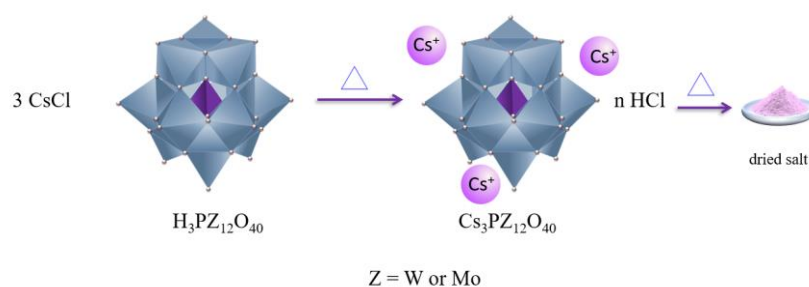
### 2.1. Synthesis of Keggin HPAs: Phosphotungstic, Phosphomolybdic and Silicotungstic Acid Cesium Salts

The most common synthesis route of Keggin HPA cesium salts starts from the reaction of an aqueous solution of commercial HPAs with another solution containing a stoichiometric amount of CsCl<sub>(aq)</sub> or Cs<sub>2</sub>CO<sub>3(aq)</sub>, which was slowly added giving a white or yellow precipitate (i.e., Cs<sub>3</sub>PW<sub>12</sub>O<sub>40</sub>, O<sub>3</sub>, Cs<sub>4</sub>SiW<sub>12</sub>O<sub>40</sub>, or Cs<sub>3</sub>PMO<sub>12</sub>O<sub>40</sub>) [35–40]. This method is named direct precipitation. After 3 h of magnetic stirring and heating to 333 K, the solution was vapoured under a vacuum releasing HCl<sub>(g)</sub>. Afterwards, the solid salt was dried in an oven at 423 K for 12 h. This procedure is depicted in Schemes 1 and 2 for the three Keggin HPAs.

It is important to note that no modification happens in the Keggin heteropolyanion structure; its integrity is preserved, and it maintains the same composition as the precursor acid; sometimes they are named saturated salts.



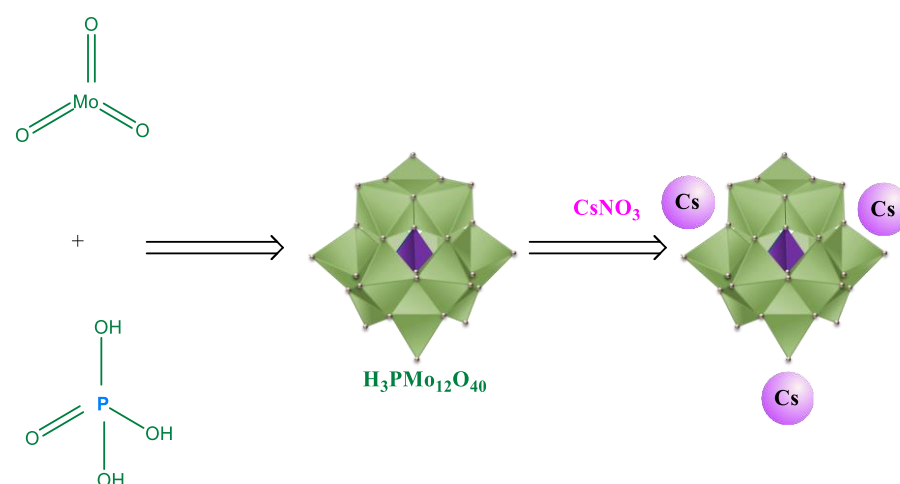
**Scheme 1.** Synthesis of cesium silicotungstate from the reaction of silicotungstic acid and cesium chloride.



**Scheme 2.** Synthesis of cesium phosphomolybdate or phosphotungstate from the reaction of phosphomolybdic acid and cesium chloride.

Another strategy is the partial replacement of protons with cesium, which generate salts with higher remaining acidity. In this case, stoichiometry is responsible for the level of exchange of protons [41]. In this review, cesium partially exchanged heteropolyacids salts had their catalytic activity addressed in Section 4 [35,36].

Beyond the direct precipitation method, there is also the reactive synthesis method [42]. Gu et al. synthesized cesium salts using the two methods and evaluated the catalysts in alkylation reactions of toluene with benzyl alcohol (Scheme 3) [43].

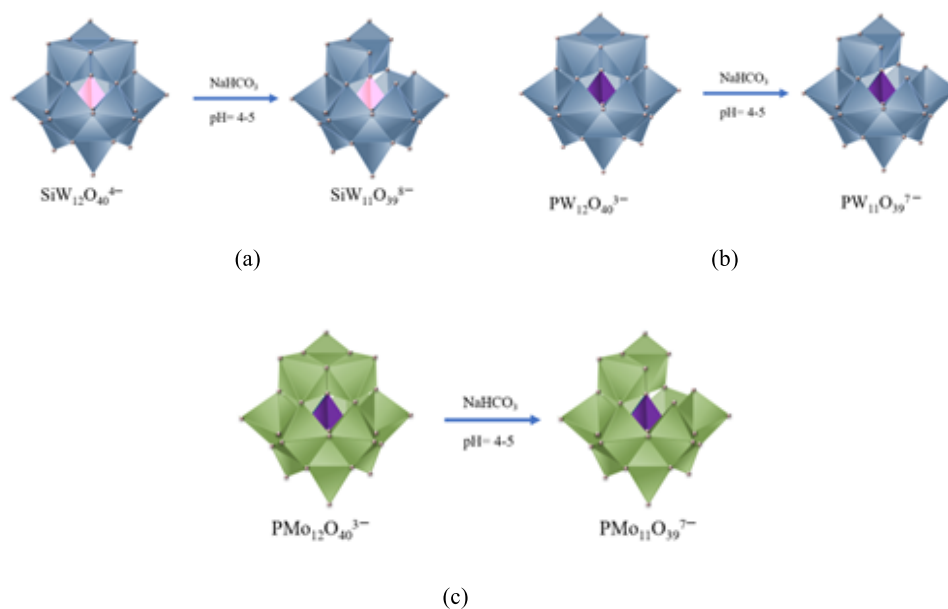


**Scheme 3.** Synthesis of cesium phosphomolybdate from the reaction of phosphoric acid, molybdenum oxide, and cesium nitrate.

Those authors heated the slurry to 100 °C for 6 h under vigorous stirring, and then evaporated to dryness at 110 °C, obtaining the  $\text{Cs}_3\text{PMo}_{12}\text{O}_{40}$  solid salt [43]. This same procedure can generate cesium phosphotungstate exchanging the molybdenum for tungsten oxide. Similarly, replacing the phosphoric acid with the silicic acid led to the obtention of cesium silicotungstate salt.

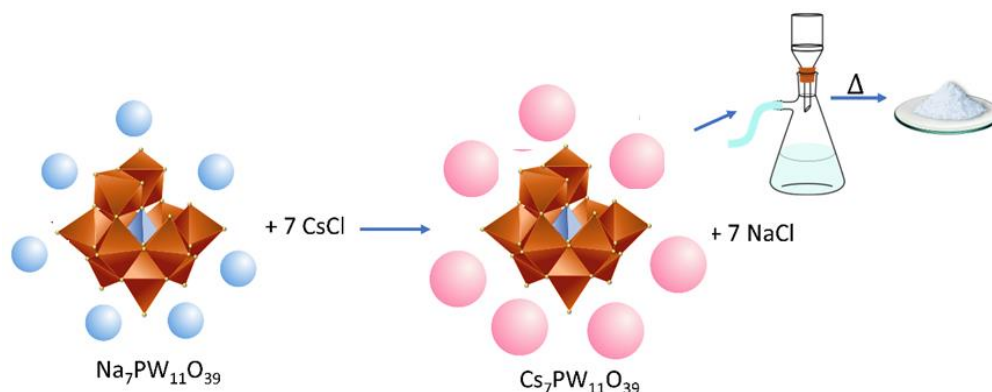
## 2.2. Synthesis of Lacunar Keggin HPA Cesium Salts

Cesium lacunar salts  $\text{Cs}_y\text{XM}_{11}\text{O}_{39}$  ( $X = \text{Si}$  or  $\text{P}$ ;  $M = \text{W}$  or  $\text{Mo}$ ;  $y = 8$  or  $7$ , respectively) have been synthesized by precipitation according to the procedure adapted from the literature [21,41]. This procedure can be carried out in a two-step synthesis. In the first procedure, the lacunar heteropolyanion is obtained by hydrolysis saturated anion present in precursor acid (Scheme 4); after the hydrolysis, the solutions of HPAs (i.e.,  $\text{H}_3\text{PW}_{12}\text{O}_{40}$ ,  $\text{H}_3\text{PMo}_{12}\text{O}_{40}$ , or  $\text{H}_4\text{SiW}_{12}\text{O}_{40}$ ) become solutions of unsaturated anions (Scheme 4).



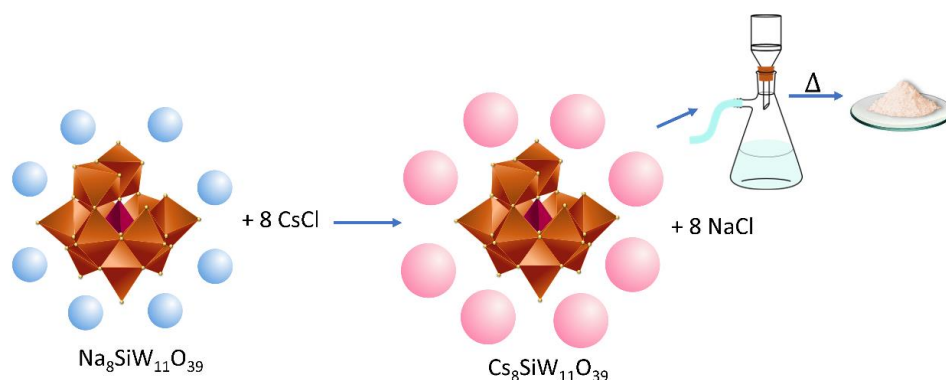
**Scheme 4.** Synthesis of lacunar silicotungstate, phosphotungstate, and phosphomolybdate anions [21,40]. (a) undecasilicotungstic anion, (b) undecaphosphotungstic anion, (c) undecaphosphomolybdate anion.

In the second stage, this lacunar anion (i.e., normally a sodium salt) reacts with a solution of cesium chloride giving a lacunar cesium heteropoly salt, which is filtered and dried in an oven (Schemes 5–7).

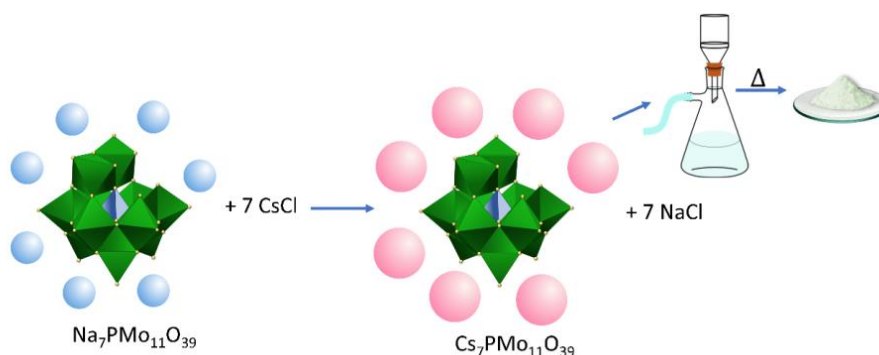


**Scheme 5.** Synthesis of lacunar cesium phosphotungstate from the reaction of lacunar sodium phosphotungstate and cesium chloride [21,41].

In these procedures, lacunar sodium salt reacts with cesium chloride giving a precipitated lacunar cesium salt, which is posteriorly filtered, and dried as in Schemes 1 and 2. Although simple, this is a two-step process: in the first, Keggin HPA is converted to the lacunar sodium salt, and in the second one, lacunar HPA cesium salt is precipitated.

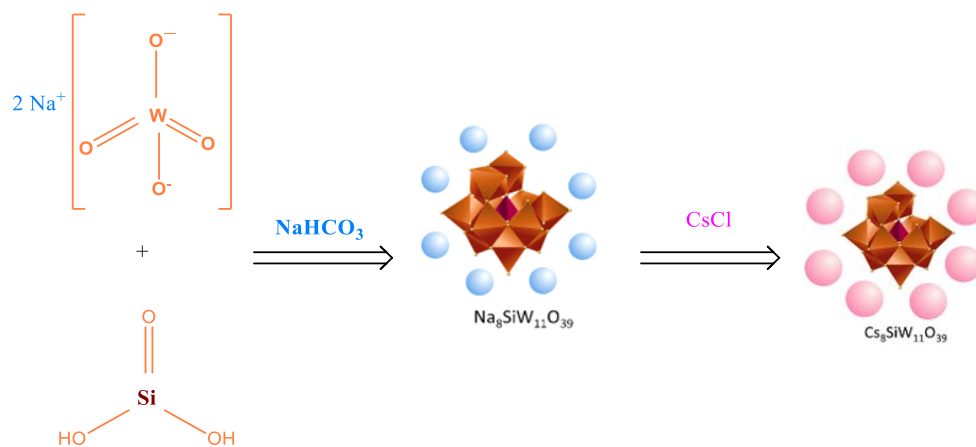


**Scheme 6.** Synthesis of lacunar cesium phosphotungstate from the reaction of lacunar sodium phosphotungstate and cesium chloride [21,41].

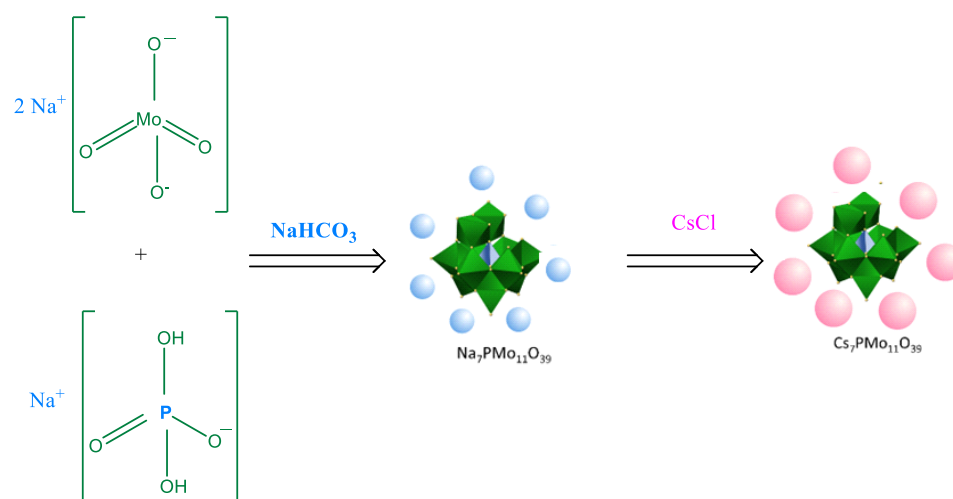


**Scheme 7.** Synthesis of lacunar cesium phosphomolybdate from the reaction of lacunar sodium phosphomolybdate and cesium chloride [21,41].

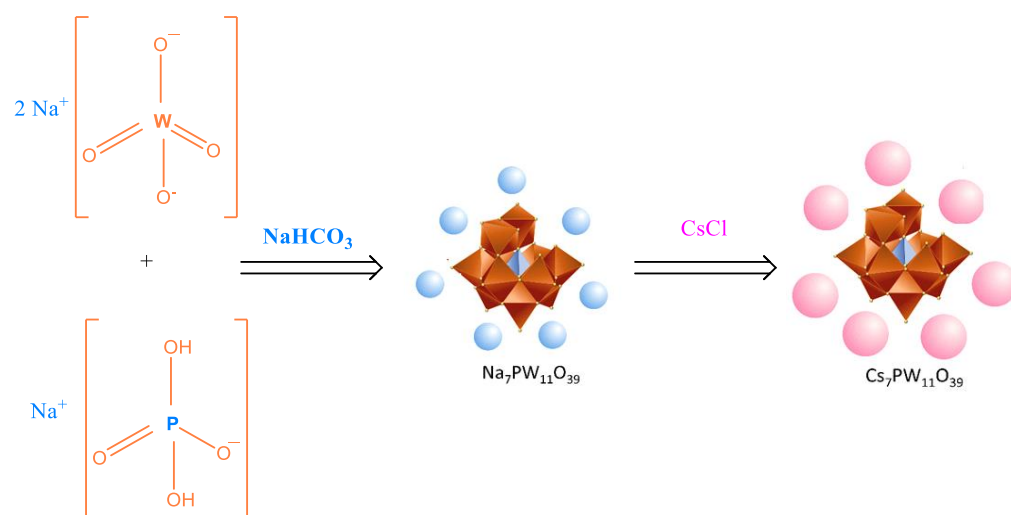
Alternatively, this route can be performed in a one-pot synthesis (Schemes 8–10). Typically, an acidic aqueous solution of the sodium tungstate or molybdate precursor (i.e.,  $\text{Na}_2\text{WO}_4$  or  $\text{Na}_2\text{MoO}_4$ ) is added to the other solution containing the silicon or phosphorus precursor salt (i.e.,  $\text{Na}_2\text{SiO}_3$  or  $\text{Na}_2\text{HPO}_4$ ), depending on the goal heteropolyanion (i.e.,  $\text{SiW}_{12}\text{O}_{40}^{4-}$ ,  $\text{PW}_{12}\text{O}_{40}^{3-}$  or  $\text{PW}_{12}\text{O}_{40}^{3-}$ ). This same procedure was previously used to synthesize lacunar potassium salts [34,44].



**Scheme 8.** One-pot synthesis of lacunar cesium silicotungstate.



**Scheme 9.** One-pot synthesis of lacunar cesium phosphomolybdate.



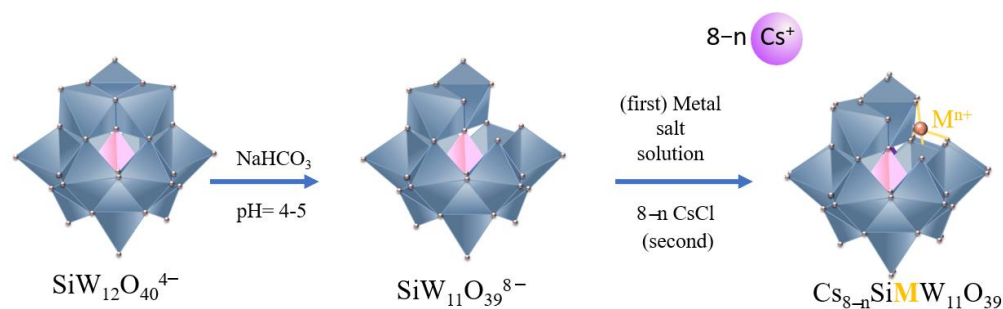
**Scheme 10.** One-pot synthesis of lacunar cesium phosphotungstate.

The addition of  $\text{NaHCO}_3$  (ca.  $0.10 \text{ mol L}^{-1}$ ) adjusted the pH to the adequate range (pH = 5.4,  $\text{SiW}_{11}\text{O}_{39}^{8-}$  and  $\text{PW}_{11}\text{O}_{39}^{7-}$ ; pH = 4.5,  $\text{PMo}_{11}\text{O}_{39}^{7-}$ ), converting the saturated anions to lacunar anions. These solutions are then stirred and heated at 353 K/60 min. Afterwards, they are cooled to room temperature, and 0.1 mol of  $\text{CsCl}_{(s)}$  is added to give precipitate the cesium HPA salt. The solid salt is washed twice (50 mL,  $1.0 \text{ mol L}^{-1}$   $\text{CsCl}_{(aq)}$ ), and once with 50 mL of cold distilled water, being then dried in air. After this step, cesium salts were dried in an oven at 423 K/5 h.

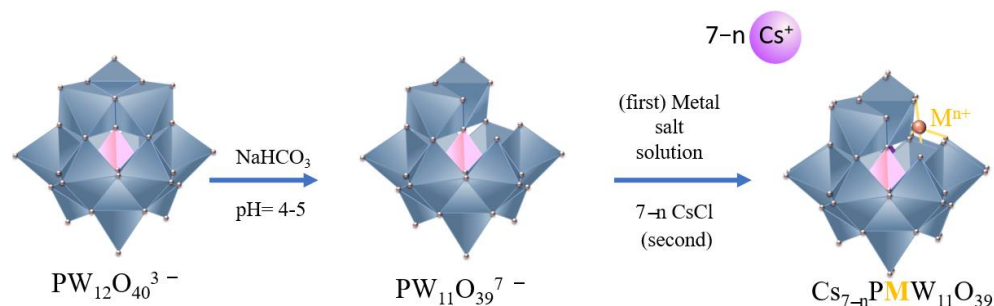
### 2.3. Synthesis of Metal-Substituted Lacunar Keggin HPA Cesium Salts

To synthesize the metal-doped cesium heteropoly salt, any one of the two procedures previously described can be used (i.e., one-pot synthesis or two-step route). Schemes 11–13 summarize the process for the three metal-doped Keggin cesium salts. However, the solution containing the precursor metal chloride must be added before the precipitation of heteropoly with  $\text{CsCl}$  [45].

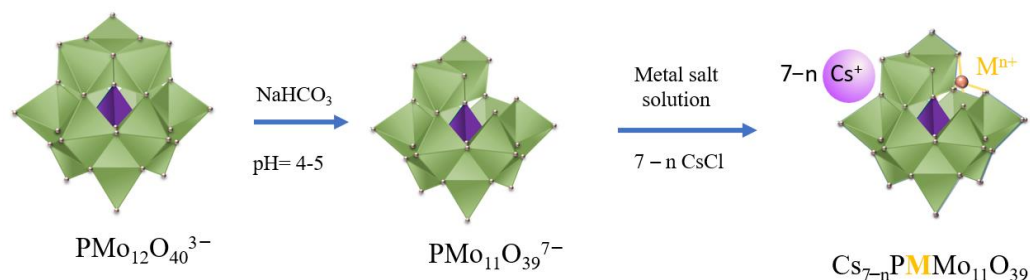
When the lacunar heteropoly sodium salt is in the solution, it acts as a “monodentate ligand” and can bind the metal cation. Therefore, the addition of  $\text{CsCl}$  precipitates this “POM complex”, which can act as a bifunctional catalyst. Besides the activity of heteropolyanion containing the addenda metal active sites (i.e., Mo or W), now the POM has yet a metal cation that frequently can trigger a synergism with the heteropolyanion, due to its catalytic activity [46].



**Scheme 11.** Metal-doped cesium silicotungstate salt.



**Scheme 12.** Metal-doped cesium phosphotungstate salt.



**Scheme 13.** Metal-doped cesium phosphomolybdate salt.

The sodium ions of  $\text{NaHCO}_3$  and chloride ions belonging to the metal or cesium chloride remain in the solution and are separated when the solid metal-doped cesium heteropoly salt is filtered. on the catalytic activity of cesium heteropoly salts.

All the cesium salts described until now (i.e., saturated, lacunar, metal-doped) demonstrated to be active catalysts in a plethora of reactions, which will be addressed in this review. However, before that, a brief discussion about the main characterization techniques could be useful to understand how they act.

### 3. Characterization Techniques of Keggin HPA Salts

There are several techniques used to characterize Keggin HPAs in a solid or liquid phase. We will focus only on the most used. The most of characterization data presented were described in the Doctorate Thesis of a researcher's group and were partially reported in the references mentioned [35–37].

#### 3.1. Infrared Spectroscopy

Infrared spectroscopy is a valuable tool to obtain information about the primary structure of Keggin HPAs (i.e., heteropolyanion). The typical chemical bonds present in the Keggin anion have their main vibrations bands placed at the fingerprint region between  $400$  to  $1300\text{ cm}^{-1}$  in the infrared spectrum. To check if the primary structure was kept constant after the synthesis of cesium salts, it needs to verify if any shoulder, new band, or

strong shift has occurred in the characteristic vibration bands of main chemical bonds after the synthesis.

The following spectra (Figure 1) were recorded in Varian 660-IR equipment with attenuated total reflectance accessory (FT-IR/ATR), in a spectral range of 550 to 1650  $\text{cm}^{-1}$ . The oxygen atoms were distinguished by subscripts as follows;  $\text{O}_a$  refers to the oxygen atom bonded to the phosphorous or silicon atom;  $\text{O}_b$  oxygen atoms belong to the  $\text{WO}_6$  or  $\text{MoO}_6$  octahedral units sharing corners;  $\text{O}_c$  oxygen atoms are in edges and  $\text{O}_d$  are terminal oxygen atoms linked to the tungsten or molybdenum atoms [35–37].

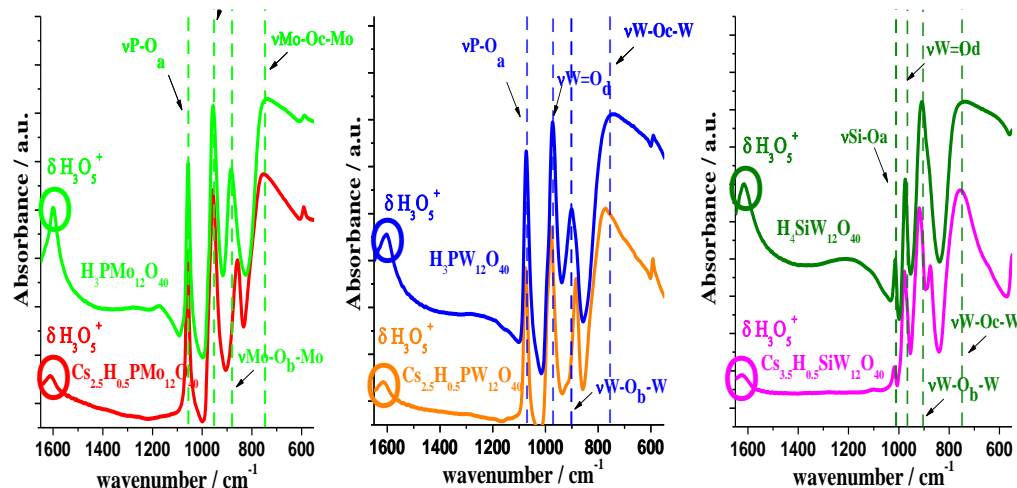


**Figure 1.** Infrared spectra of phosphotungstic, phosphomolybdic, and silicotungstic acids and their partially-exchanged cesium salts (adapted from refs. [35–37]).

A comparison of typical absorption bands of the pristine Keggin HPAs with their partially cesium-exchanged salts allows concluding that only the absorption bands assigned to the vibration of  $\text{W}(\text{Mo})\text{-O}_b\text{-W}(\text{Mo})$  bonds of cesium salts were shifted toward a lower wavenumber. This effect can be assigned to the weakening of  $\text{W}(\text{Mo})\text{-O}$  chemical bonds triggered by the cesium cations.

The impacts of the substitution level of cesium on the infrared spectra of phosphotungstate salts were also evaluated (Figure 2). An increase in cesium load has not triggered any noticeable change in the wavenumber of typical absorption bands of cesium salts in the range of 0.5 to 3.0 mol  $\text{Cs}^+$ /mol heteropolyanion.

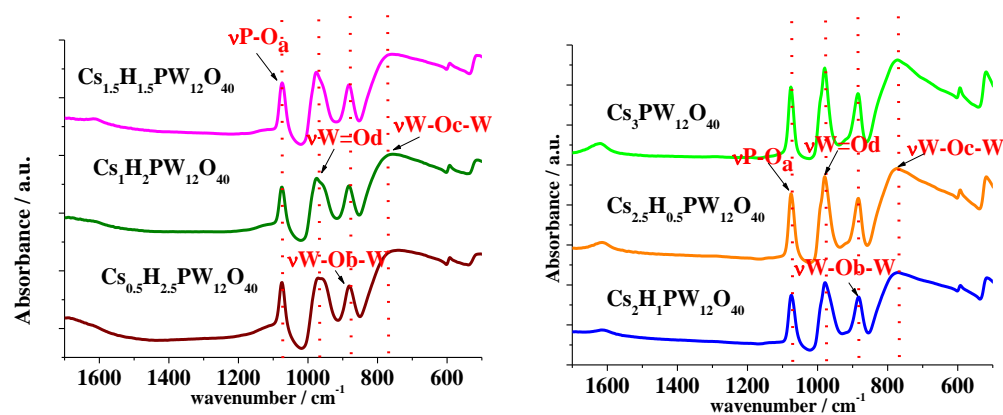


**Figure 2.** Impact of cesium load on the infrared spectra of cesium phosphotungstate salts (Adapted from refs. [35–37]).



### 3.2. Powder XRD Patterns

The powder X-rays diffraction patterns of the cesium salts of silicotungstic, phosphomolybdic, and phosphotungstic acids were obtained by X-ray diffraction (XRD) in a Bruker D8 Discovery diffractometer, operating at 40 kV acceleration voltage, 40 mA current, in the copper emission line (Cu-K $\alpha$ ,  $\lambda = 1.5406 \text{ \AA}$ ), with a scanning rate of  $1^\circ / \text{min}$  for a  $2\theta$  angle of  $5\text{--}80^\circ$  [35–37]. The diffractograms of Keggin heteropolyacids and their cesium salts are displayed in Figure 3.

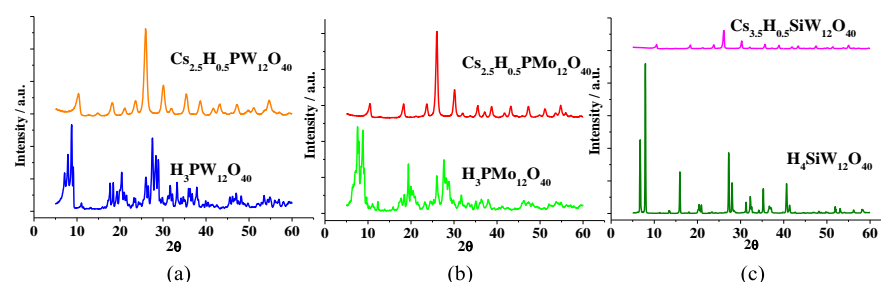


**Figure 3.** Powder XRD patterns of phosphotungstic (a), phosphomolybdic (b), silicotungstic acids (c), and their cesium-partially exchanged salts (adapted from refs. [35–37]).

The diffractograms of phosphotungstic and phosphomolybdic acid cesium salts had diffraction peaks in a higher amount and were well-defined than pristine HPAs. Despite the similar profile, at a low angle  $2\theta$  angle ( $<10^\circ$ ) the Keggin HPAs diffractograms presented high-intensity peaks, which are characteristic of them; conversely, the XRD patterns of cesium salts have not displayed these strong peaks at this region.

From the Scherrer Equation (1), it is possible to calculate the crystallite size of a solid particle of Keggin HPAs and their cesium salts. In Equation (1),  $\lambda$  is the X-ray wavelength (nm),  $\beta$  is the peak width of the diffraction peak profile at half maximum height resulting from small crystallite size in radians, and  $K$  is a constant related to crystallite shape, normally taken as 0.89.

$$L = \frac{K \cdot \lambda}{\beta \cdot \cos\theta} \quad (1)$$

In Figure 4, it is possible to see that the doping with cesium led to a lower crystal size, mainly when comparing the silicotungstic acid with the cesium silicotungstate.

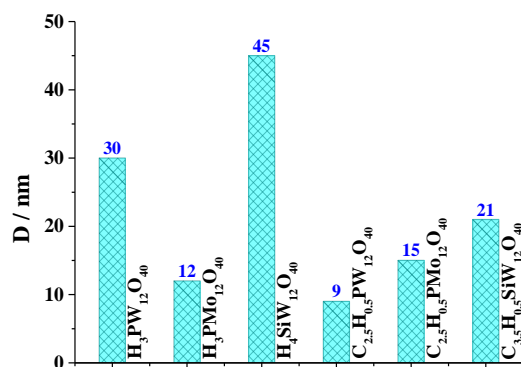


**Figure 4.** The crystallite size of phosphotungstic, phosphomolybdic, and silicotungstic acids and their cesium-partially exchanged salts (adapted from refs. [35–37]).

The greatest crystallite size of silicotungstic acid is confirmed by their diffractogram, which presented the most intense diffraction line close to  $9.0^\circ$   $2\theta$  angle. Figure 5 shows the impact of the increase in cesium load on the crystallite size for the phosphotungstate catalysts.

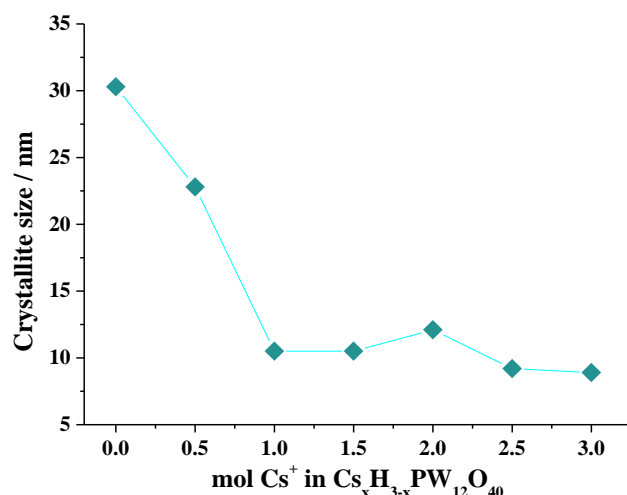


**Figure 5.** Impact of cesium load on the crystallite size of cesium phosphotungstate salts.

An increase in cesium load until 1.0 mol Cs<sup>+</sup>/mol heteropolyanion provokes a diminishment in the crystallite size; after this proportion, no significant effect was verified when more cesium was included in heteropoly salts.

### 3.3. Thermal Analyses

Thermogravimetric analysis (TG–DSC) allows us to investigate the thermic stability of catalysts and determine the number of hydration water molecules. The data described herein were acquired in a Perkin Elmer simultaneous thermal analyzer (STA) 6000, using 10 mg of sample in a standard alumina crucible. The sample was heated from 298 to 973 K with a rate of 10 K min<sup>−1</sup> under nitrogen flow. Figure 6 displays results obtained from phosphotungstic, phosphomolybdic, and silicotungstic acids and their cesium-partially exchanged salts.

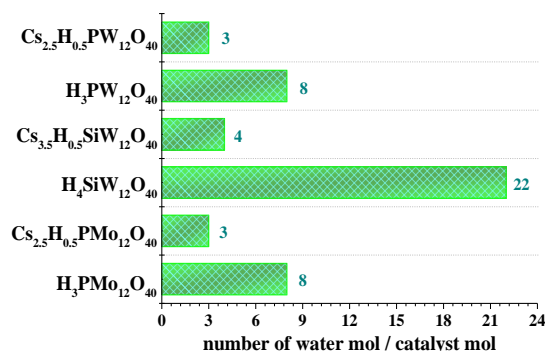


**Figure 6.** The number of waters mol per catalyst mol of the phosphotungstic, phosphomolybdic, and silicotungstic acids and their cesium-partially exchanged salts was determined through TG analysis (adapted from refs. [35–37]).

Regardless of the Keggin anion, the HPAs always presented a hydration level greater than cesium salts. It is a consequence of the thermal treatment procedure undergone by the cesium salts after the synthesis.

Figure 7 shows the effect of cesium load on the number of hydration water molecules. An increase in cesium load resulted in a lower number of water molecules per mol of heteropolyanion. It can be a consequence of the great ionic radius of cesium; the higher the cesium content, the more difficult was for the water molecules to interact with the Keggin anion, and, consequently, lower the hydration level.

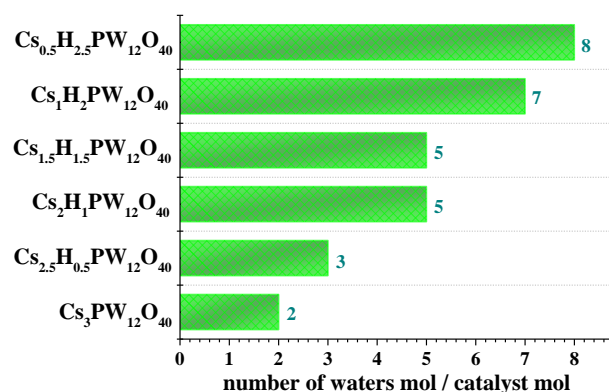


**Figure 7.** The number of water mol per catalyst mol of cesium phosphotungstate salts (adapted from refs. [35–37]).

### 3.4. Surface Area: Brunauer–Emmett–Teller (BET) Method

To be an effective heterogeneous catalyst, the solid should have a high surface area and adequate porosity, allowing the reactant molecules to interact, with the help of active sites, leading to the formation of a goal product with high conversion and selectivity. Herein, the surface area of Keggin HPAs and their cesium salts were analyzed by the Brunauer–Emmett–Teller (BET) method, and the diameters and distribution of pore volumes were calculated according to the Functional Density Theory (DFT). These analyses were carried out on NOVA 1200 Quantachrome, through the isotherms of physical adsorption/desorption of  $\text{N}_2$ , at 77 K [35–37]. Figure 8 shows the BET surface area of phosphomolybdic acid and their cesium salts.

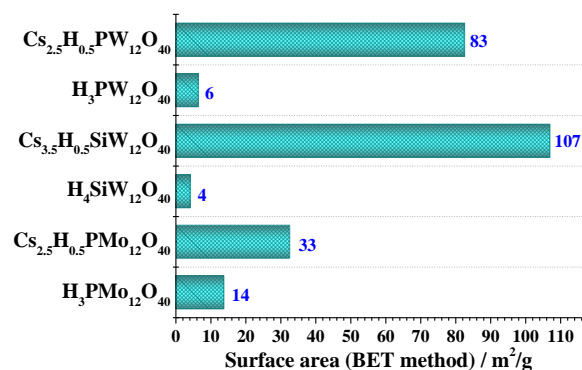


**Figure 8.** Surface area (BET) of phosphotungstic, phosphomolybdic, and silicotungstic acids and their cesium-partially exchanged salts (adapted from refs. [35–37]).

Remarkably, the surface area of cesium salts was much greater than pristine Keggin HPAs [35–37,40]. It is in accordance with the literature [39,41]. This effect was more noticeable in the tungsten catalysts.

The impacts of cesium load on the surface area of cesium phosphotungstate salts catalysts were assessed the main results are displayed in Figure 9. In general, an increase in cesium load had a positive effect on the surface of tungsten heteropoly salts.

However, for lower cesium content the increase in surface area was less impacted. Conversely, when 2.0 or more Cs mol were present in the heteropolyanion, the surface was remarkably enhanced (Figure 10).

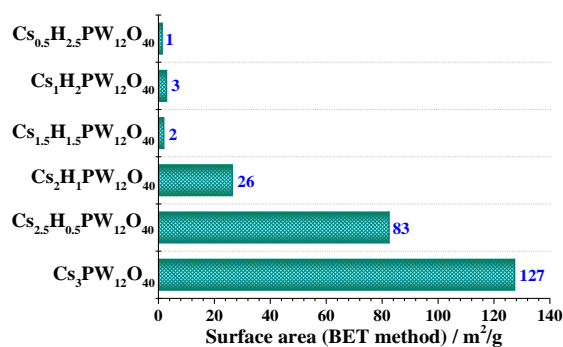


Figure 9. Surface area (BET) of cesium phosphotungstate salts (adapted from refs. [35–37]).

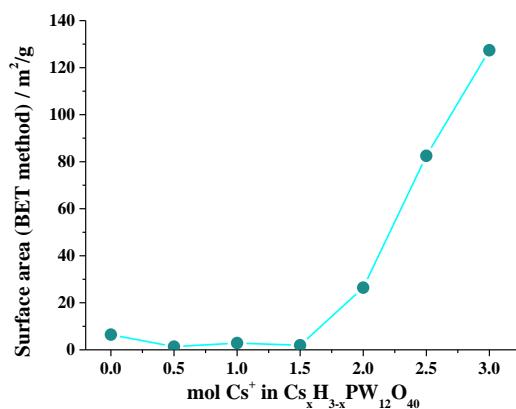


Figure 10. Impact of cesium load on the surface area (BET) of cesium phosphotungstate.

The nitrogen adsorption/desorption isotherms provide valuable information about the surface area and porosity of cesium heteropoly salts. However, Hyhoshi and Kamyhia observed the microstructure from micropores using aberration-corrected scanning transmission electron microscopy [47]. Those authors verified that although silicotungstic and phosphotungstic acids are solids with a low surface area when their protons are exchanged with cesium, rubidium, or ammonium, their surface area and porosity properties are strongly improved. They conclude the cesium content controls the pore size and pore-size distributions, using high-resolution imaging through transmission electron microscopy (TEM) and scanning transmission electron microscopy (STEM). These techniques provide direct evidence for the structures of defects and interfaces. Moreover, they used aberration-corrected TEM and STEM for atomic-scale observations. Different microstructures that form micropores of Cs<sub>2.5</sub>H<sub>1.5</sub>SiW<sub>12</sub>O<sub>40</sub> and Cs<sub>4.0</sub>SiW<sub>12</sub>O<sub>40</sub> were visualized by using aberration-corrected STEM. Those authors demonstrated the presence of microstructures that form the microporosity of Cs<sub>2.5</sub>H<sub>1.5</sub>SiW<sub>12</sub>O<sub>40</sub> salt and anion vacancies in both salts (i.e., Cs<sub>2.5</sub>H<sub>1.5</sub>SiW<sub>12</sub>O<sub>40</sub>, Cs<sub>4.0</sub>SiW<sub>12</sub>O<sub>40</sub>).

### 3.5. Measurements of Acidity Strength of Cesium Heteropoly Salts

The number and strength of the acid sites of the Cs<sup>+</sup> exchanged phosphotungstic acid salts were determined by *n*-butylamine potentiometric titration using a BEL potentiometer, model W3B, with a glass electrode [35–37]. For comparison, the acidity of the pristine heteropolyacid was also evaluated. To do it, a solid salt (ca. 50 mg) was suspended in CH<sub>3</sub>CN (30 mL) and magnetically stirred for 3 h. Posteriorly, the suspension was slowly titrated with *n*-butylamine solution (portions of ca. 100 μL, 0.025 mol L<sup>-1</sup>), until the electrode potential kept stable after the addition of the titrant.

Figure 11 show the initial electrode potential values obtained from the solution or suspension of phosphotungstic catalysts. As expected, the solution of H<sub>3</sub>PW<sub>12</sub>O<sub>40</sub> and the suspension of Cs<sub>3</sub>PW<sub>12</sub>O<sub>40</sub> salt presented the highest and the lowest acidity, as showed the

Ei values measured. Nonetheless, the strength of acidity of other cesium salts randomly varied, with values between 562 to 638 mV.

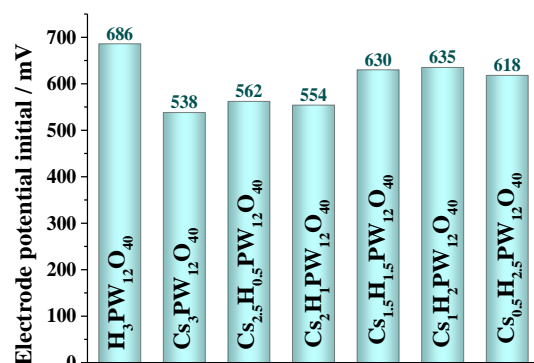


**Figure 11.** The initial electrode potential of suspensions in acetonitrile of the cesium phosphotungstate salts and solution of precursor phosphotungstic acid (adapted from ref. [36]).

Figure 12 shows the effect of cesium load on the acid site's number of cesium phosphotungstate catalysts.

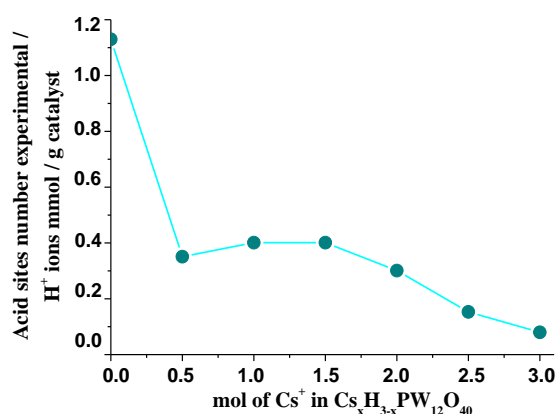


**Figure 12.** Effect of cesium load on the acid sites number of the cesium phosphotungstate salts and phosphotungstic acid.

The partial replacement of protons in Keggin-type HPAs with larger cations can make them insoluble in water. Although the amount of Brønsted acid sites in  $\text{Cs}_x\text{H}_{3-x}\text{PW}_{12}\text{O}_{40}$  became lower as compared to  $\text{H}_3\text{PW}_{12}\text{O}_{40}$ , the strength of Brønsted acidity for  $\text{Cs}_x\text{H}_{3-x}\text{PW}_{12}\text{O}_{40}$  was still preserved [48]. When Keggin HPAs are compared to the typical inorganic acids, their greater acidity is ascribed to the size and charge of the anion [49]. However, even cesium is included in the secondary structure of HPAs, these cations can be hydrolyzed generating  $\text{H}^+$  ions that contributes to the acidity of salts [50] and, thus, weaken the attraction of the proton to the anion.

#### 4. Keggin HPA Cesium Salts-Catalyzed Reactions

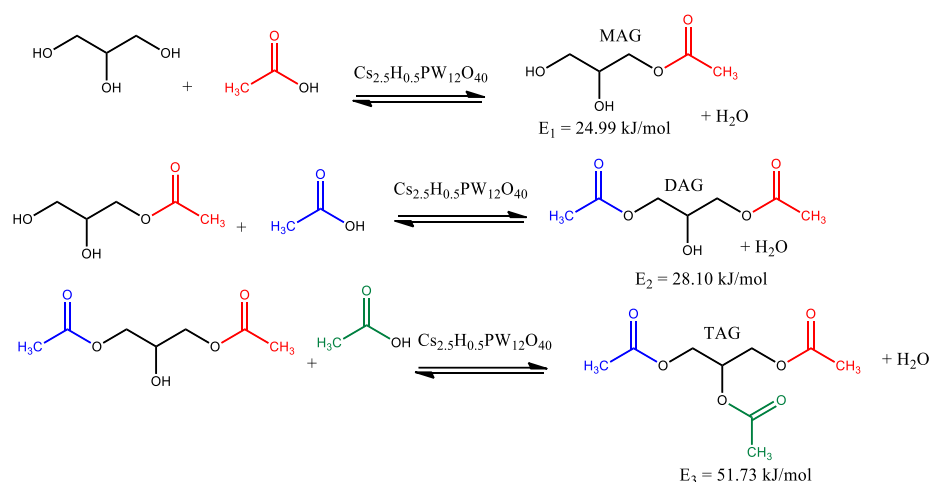
Keggin HPA cesium salts are versatile catalysts active in different reactions such as those acid-catalyzed (i.e., esterification, etherification, acetalization, ketalization, hydrolysis) or oxidative transformations (i.e., desulfurization, oxidation of alcohols, aldehydes, and olefines). In this review, we will try to separately address these two types of reactions.

##### 4.1. Keggin HPA Cesium Salts: Acid-Catalyzed Reactions

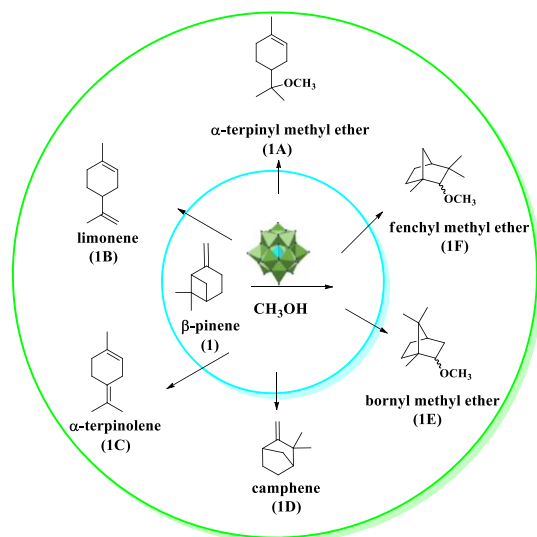
Nowadays, glycerol esters and ethers have been considered potential bioadditives to be blended with fossil fuels, consequently, a growing interest in the development of synthesis processes of these oxygenated compounds from glycerol generated in surplus by

the biodiesel industry has been observed [51]. The blending of these glycerol-derived with diesel improves internal combustion efficiency, decreases greenhouse gas emissions, and increases fuel properties such as cetane number and cloud points [52,53].

In this sense, Veluturia et al. studied the glycerol esterification over cesium partially exchanged phosphotungstic acid salts [54]. Scheme 14 shows the main reaction products of glycerol esterification; the terminal hydroxy groups are preferentially esterified. Consequently, monoacetyl glycerol, 1,3-diacetyl glycerol, and triacetyl glycerol are the main products (i.e., MAG, DAG, and TAG, respectively). The reactions were carried out over a partially exchanged-cesium phosphotungstate ( $\text{Cs}_{2.5}\text{H}_{0.5}\text{PW}_{12}\text{O}_{40}$ ). Those authors determined through kinetic study that this reactivity sequence is a consequence of trends observed in the activation energy of these reactions (Scheme 15).



**Scheme 14.** The activation energy of formation reactions of MAG, DAG, and TAG (adapted from ref. [54]).



**Scheme 15.** Main products of Keggin HPAs-catalyzed reactions of  $\beta$ -pinene with methyl alcohol over  $\text{Cs}_{2.5}\text{H}_{0.5}\text{PW}_{12}\text{O}_{40}$  [36].

Terpenes are renewable, abundant, and inexpensive raw materials, which can be valorized by modifying their chemical structure and consequent conversion to compounds that have industrial applications such as polymers, solvents, pharmacies, and fragrances [47]. In this sense, the development of processes to convert monoterpenes into fine chemicals with a higher value-added has been a goal of several research groups.

In particular, terpene ethers are compounds used as traction fluid, or in the field of fragrance and solvents. In addition, terpene ethers are bioactive compounds with antimicrobial and food preservative properties that are considered as a real potential application in the food industry [55].

In this regard, partially exchanged cesium salts were also effective catalysts in monoterpenes etherification reactions with alkyl alcohols [36]. Da Silva et al. carried out the  $\beta$ -pinene etherification with methyl alcohol and verified that at those conditions, the monoterpene substrate undergoes skeletal rearrangement reactions giving mainly  $\alpha$ -terpinyl methyl ether (1A) as the main product (Scheme 15). This is a product of the nucleophilic addition of methyl alcohol to the tertiary carbocation resulting from the opening of the four-membered ring of  $\beta$ -pinene.

Typically, the catalytic tests were performed in a glass reactor (25 mL) fitted with a sampling septum and under magnetic stirring, containing  $\beta$ -pinene (3.74 mmol), solved in alkyl alcohol (10 mL), heated to 333 K temperature.

Although a high selectivity toward  $\alpha$ -terpinyl methyl ether (1A) has been achieved (60%), other two types of products were also formed: fenchyl (1F) and bornyl (1E) methyl ethers, which were also resulting from the rearrangement of carbon skeletal followed by nucleophilic addition of methyl alcohol, and, secondly, isomerization products, such as camphene (1D), limonene (1B),  $\alpha$ -terpinolene (1C). Figure 13 displays the conversion and selectivity reached in the reactions in the presence of Keggin HPAs or their cesium salts.

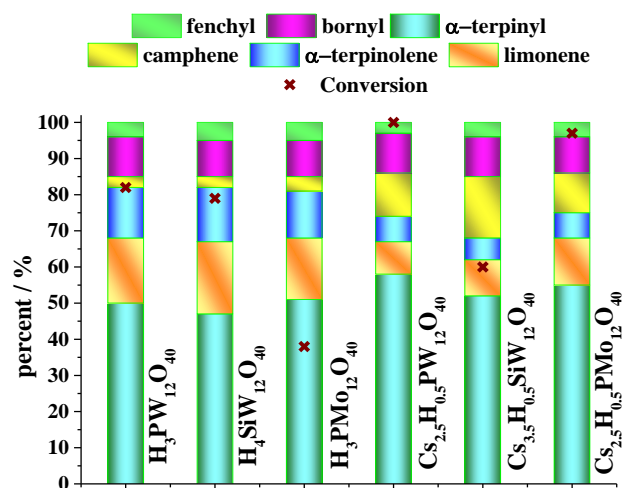
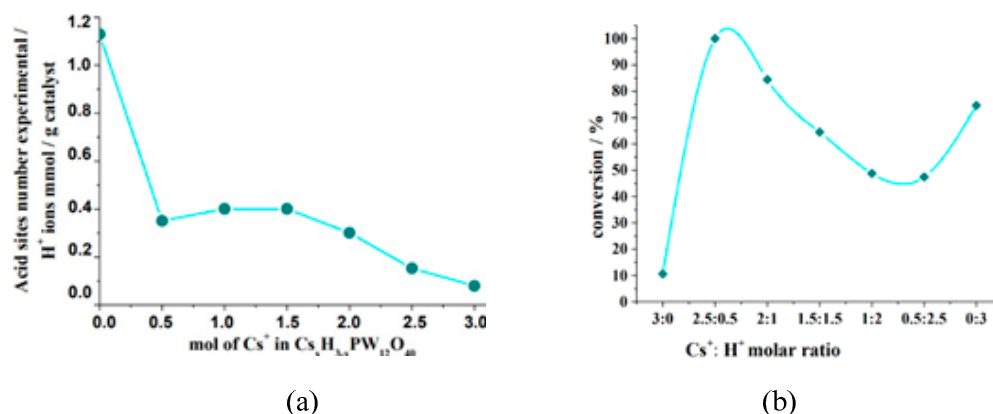


**Figure 13.** Conversion and selectivity of Keggin HPAs or their cesium salts-catalyzed reactions  $\beta$ -pinene reaction with methyl alcohol (adapted from ref. [36]).

The reaction in the presence of  $Cs_{2.5}H_{0.5}PW_{12}O_{40}$  salt achieved the highest conversion and selectivity toward  $\alpha$ -terpinyl methyl ether (1A). This result was superior to that achieved in the presence of phosphotungstic acid, which takes place in a homogeneous phase.

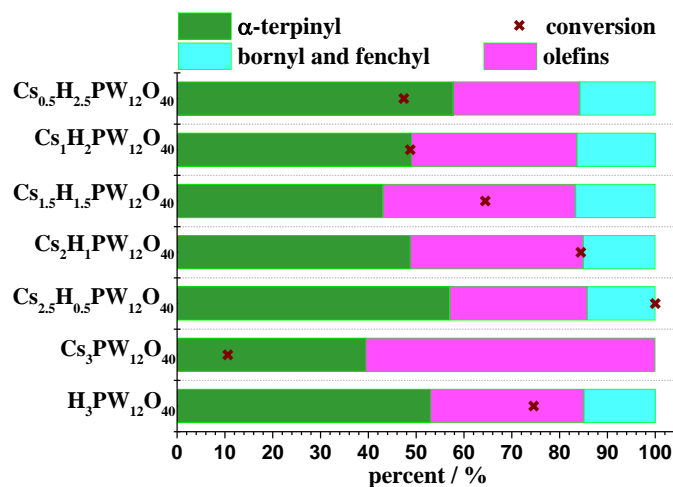
Figure 14 unequivocally shows that there is an optimum proportion between  $Cs^+$ :  $H^+$  cations. This means that an excess of protons is prejudicial for the reaction; conversely, in the absence of protons (i.e.,  $Cs_3PW_{12}O_{40}$ ), only a poor conversion was attained.

Figure 14a shows that if a high acid sites number is present (i.e.,  $H_3PW_{12}O_{40}$ ), a high conversion is achieved. However, in this case, the catalyst is soluble. Moreover, it is possible to note that the presence of a minimum amount of  $H^+$  ions is required for the success of the catalyst (Figure 14b). It is noteworthy that the leaching of the catalyst is impacted by the cesium load. If a low cesium content is present, the catalyst is more soluble.



**Figure 14.** Effect of cesium load on the phosphotungstate salts on the conversion of  $\beta$ -pinene reaction with methyl alcohol (adapted from ref. [36]).

The impacts of cesium load on the conversion and selectivity of  $\beta$ -pinene reactions with methyl alcohol were also evaluated (Figure 15). This effect was evaluated for phosphotungstate catalysts. An increase in Cs load (i.e., 0.5 to 2.5 mol of Cs/mol catalyst) increased the reaction conversions. Nonetheless, the Cs<sub>3</sub>PW<sub>12</sub>O<sub>40</sub>-catalyzed reaction reached the lowest conversion. There is no direct relation between the cesium load and reaction selectivity, however, it is possible to conclude that the 2.5:0.5 proportion of Cs: H is that that provided the highest selectivity to goal product ( $\alpha$ -terpinyl methyl ether (1A)).

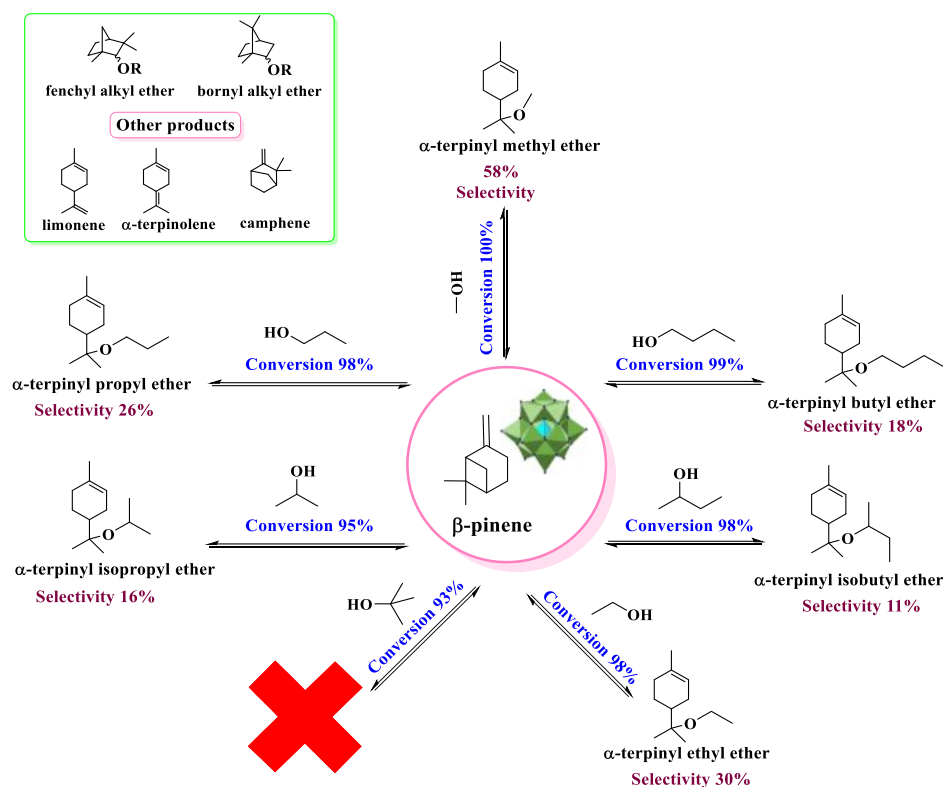


**Figure 15.** Effect of cesium load present in the phosphotungstate salts on the conversion and selectivity of  $\beta$ -pinene reactions with methyl alcohol (adapted from ref. [36]).

The Cs<sub>2.5</sub>H<sub>0.5</sub>PW<sub>12</sub>O<sub>40</sub>-catalyzed etherification reactions of  $\beta$ -pinene were carried with different alcohols (Scheme 16). High conversions, greater than 90%, were achieved regardless of the alcohol used. The reaction selectivity to terpinyl alkyl ether had a linear behaviour concerning the size of the carbon chain of alcohol: C1, C2, C3, and C4 alcohols give 58%, 30%, 26% and 18% of selectivity. Although less reactive than primary alcohols, secondary ones also provided terpinyl alkyl ether. Only the reaction with *tert*-butyl alcohol did not give terpinyl ether.

The reusability of Cs<sub>2.5</sub>H<sub>0.5</sub>PW<sub>12</sub>O<sub>40</sub> was also evaluated (Figure 16). This catalyst was successfully recovered and reused three times in  $\beta$ -pinene reactions with methyl alcohol without loss of activity or selectivity.





**Scheme 16.** Impacts of alcohol on the conversion and selectivity of  $\text{Cs}_{2.5}\text{H}_{0.5}\text{PW}_{12}\text{O}_{40}$ -catalyzed  $\beta$ -pinene reactions (adapted from ref. [36]).

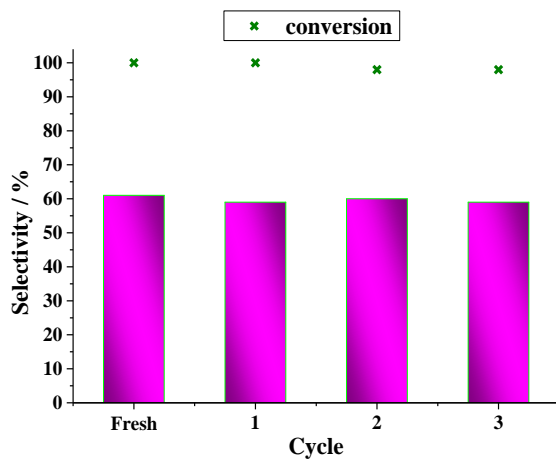


**Figure 16.** Conversions and selectivity toward  $\alpha$ -terpinyl methyl ether achieved in successive cycles of recovery and reuse of  $\text{Cs}_{2.5}\text{H}_{0.5}\text{PW}_{12}\text{O}_{40}$  catalyst in  $\beta$ -pinene reactions with methyl alcohol (adapted from ref. [36]).

Furfural is a valuable platform molecule readily accessible from biomass. It is the main unsaturated chemical obtained in large-volume from biomass resources. Their derived are essential to produce potential candidates to replace the fossil origin chemicals, with an annual production of about 300,000 t/year [56,57].

The furfural chemistry is well established, and various derived have been widely used in the industry, such as furfuryl alcohol, 5-hydroxymethyl furfural, decarbonylation products such as furan and tetrahydrofuran, and condensation products of furfural with alcohols [58,59].

This set of cesium catalysts was evaluated in furfural acetalization reactions with alkyl alcohols [35]. Furfuryl acetals are valuable ingredients of synthesis and can be used as solvents

or bioadditives. Figure 17 shows the conversion achieved in furfural acetalization reactions with methyl alcohol carried out over Keggin HPAs or their cesium-exchanged salts.

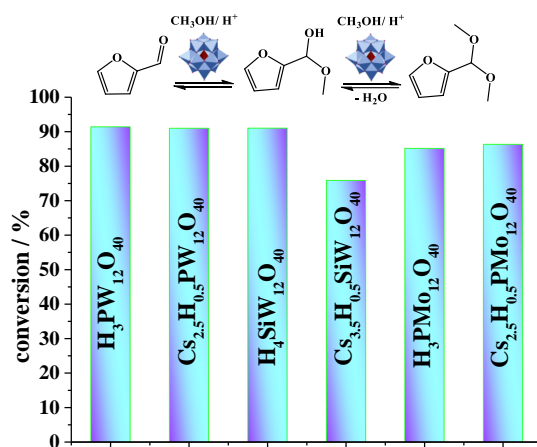


**Figure 17.** Furfural acetalization reactions with methyl alcohol in the presence of Keggin HPAs or their cesium-exchanged salts (adapted from ref. [35]).

Typically, the catalytic tests were carried out in a glass reactor (25 mL) fitted with a sampling septum, under a magnetic stirrer, containing furfural and adequate alcohol. The reactor temperature was adjusted to 298 K. Then, the reaction was started by adding of solid catalyst [35].

Different from reactions with  $\beta$ -pinene, where various products were formed, herein regardless of Keggin HPA or cesium salt only dimethyl furfuryl acetal was selectively obtained.

The reactions in the presence of the phosphotungstic catalysts (i.e., acid and cesium salt) reached the highest conversion, besides the silicotungstic acid-catalyzed reaction. However, only the  $Cs_{2.5}H_{0.5}PW_{12}O_{40}$  act as a heterogeneous catalyst, while the heteropolyacids are soluble. For this reason, it was selected to evaluate other reaction parameters.

The effect of cesium load was assessed, and the main results are presented in Figure 18. It is possible to see that the reaction conversions were not significantly affected by the cesium load present in the catalyst.

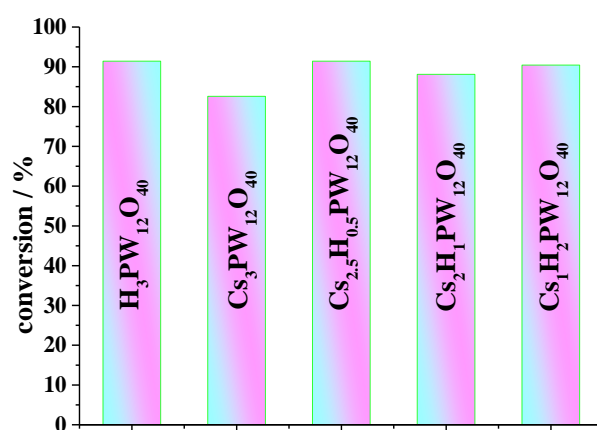


**Figure 18.** Effect of cesium load present in the phosphotungstate salts on the conversion and selectivity of furfural condensation reactions with methyl alcohol (adapted from ref. [35]).

Different from those observed in etherification reactions of  $\beta$ -pinene with methyl alcohol, the  $Cs_3PW_{12}O_{40}$  salt was also an efficient catalyst in the condensation reaction of furfural with this alcohol [35,36].

To evaluate the dependence of reaction concerning the catalyst load, a series of runs were performed, and the results are displayed in Figure 19. It is possible to see that even in

the absence of catalyst, the conversion achieves 20%. It can be explained due to the alcohol excess, which shift the equilibrium toward products even without catalyst.

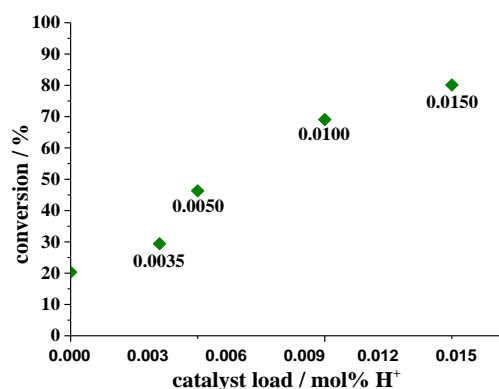
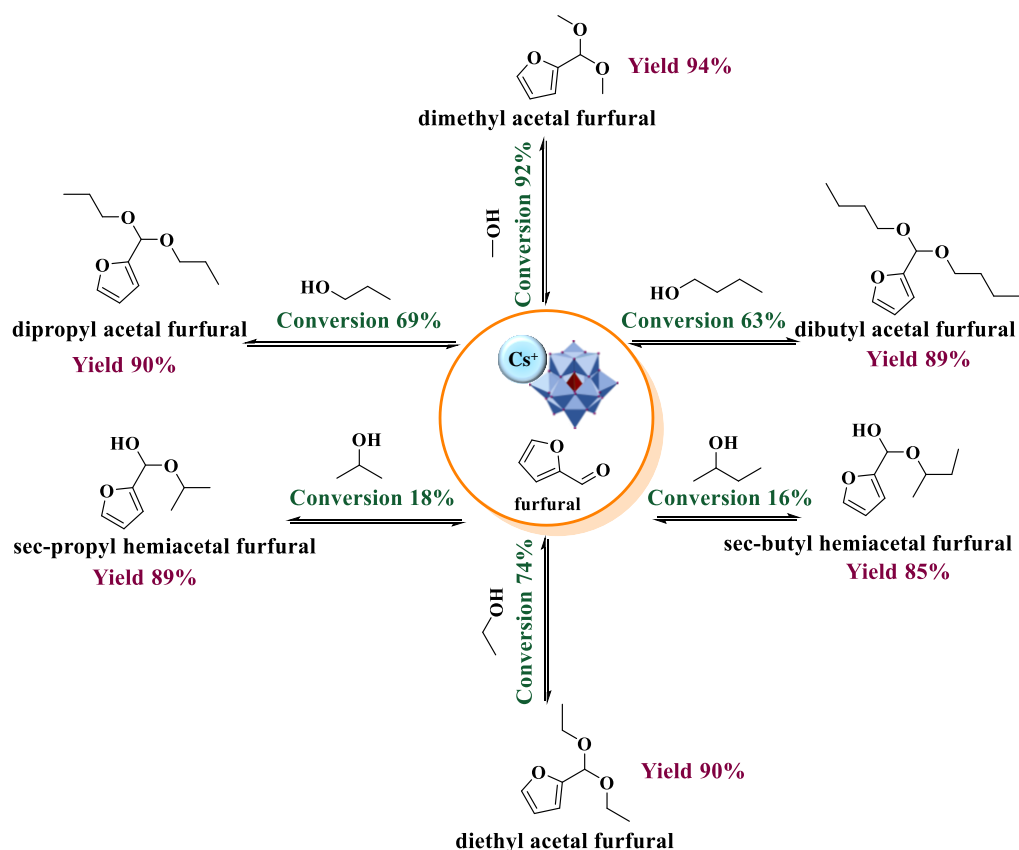


**Figure 19.** Effect of catalyst load (mol % H<sup>+</sup>) on the conversion of Cs<sub>32.5</sub>H<sub>0.5</sub>PW<sub>12</sub>O<sub>40</sub>-catalyzed furfural condensation reactions with methyl alcohol (adapted from ref. [35]).

An increase in catalyst load had a beneficial impact on the conversion; the trends observed suggest a first-order dependence concerning H<sup>+</sup> load (Figure 19).

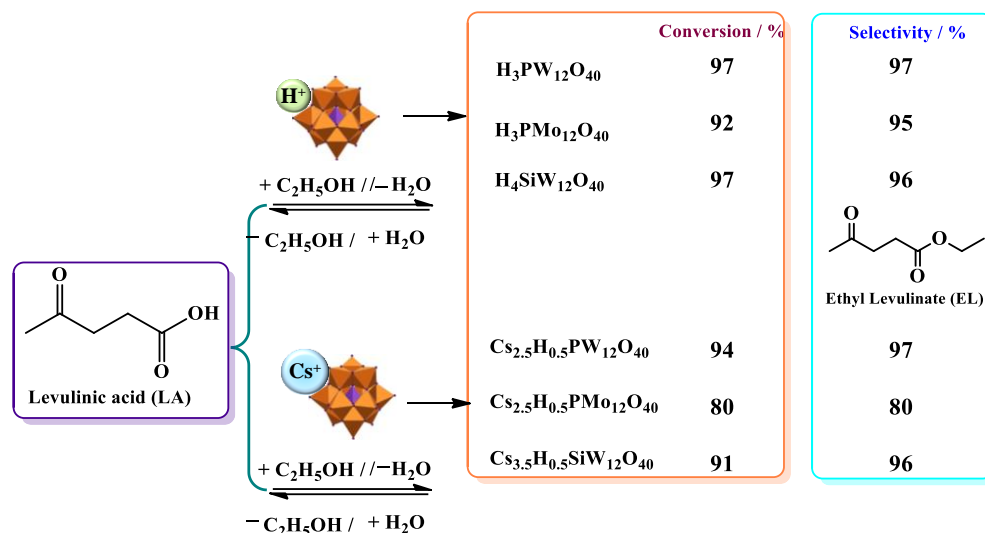
The Cs<sub>2.5</sub>H<sub>0.5</sub>PW<sub>12</sub>O<sub>40</sub>-catalyzed furfural condensation reactions were also performed with other alkyl alcohols (Scheme 17).



**Scheme 17.** Impacts of alcohol on the conversion and selectivity of Cs<sub>2.5</sub>H<sub>0.5</sub>PW<sub>12</sub>O<sub>40</sub>-catalyzed furfural condensation reactions (adapted from ref. [35]).

Different from verified in the β-pinene reactions with different alcohols, the conversions were affected by the alcohol nature. An increase in the size of the carbon chain harmed the reaction conversions; the reactions with C1, C2, C3, and C4 alcohols, achieved

92%, 74%, 69%, and 63% conversions, with furfuryl alkyl acetal yields of 94%, 90%, 90%, and 89% (Scheme 18). Due to the high steric hindrance, the secondary alcohols were less reactive, and the conversions achieved with *sec*-propyl and *sec*-butyl alcohols were 18% and 16%, respectively. In addition, different from primary alcohols, the reaction was not complete; it was stopped when the hemiacetal was obtained. It is also a consequence of steric hindrance on the hydroxyl group of alcohol.



**Scheme 18.** Esterification reactions of levulinic acid with ethyl alcohol in the presence of Keggin HPAs or their partially-exchanged cesium salts (adapted from ref. [37]).

Levulinic acid (LA) is a chemical obtained from biomass classified as one of the most promising building blocks of biorefinery, selected as one of the “Top 10” platform chemicals [60]. LA is obtained through dehydration in acidic media of hexoses (i.e., acid treatment of agricultural wastes and wastes of wood containing cellulose or hemicellulose), which gives HMF that is subsequently hydrated. It is useful as a solvent, antifreeze, resin, food flavouring agent, plasticizer, and starting material for the preparation of a variety of industrial and pharmaceutical compounds [52]. Angelica lactone, succinic acid, 1,4-pentanediol, and methyl THF are only some examples of their valuable LA derived.

Beyond these products, esters of LA are also key compounds used in the production of flavours, solvents, and plasticizers [61]. Moreover, the resulting ketoesters of the cyclization of LA are substrates for a diversity of condensation and addition reactions [62]. LA esters have properties that make them potential oxygenate additives to fossil fuels, improving their octane and cetane numbers [63,64].

The typical catalysts used for LA esterification are mineral liquid acids such as sulfuric and hydrochloric acids, however, serious drawbacks of these inexpensive catalysts are the tedious work-up procedure, the steps of neutralization and purification that result in large effluents generation, besides the difficult catalyst regeneration [65]. For these reasons, solid catalysts are preferable due to their easy separation, recycling, and lower corrosiveness [66].

Most of the time solid-supported catalysts are the option, nonetheless, the water generated as a co-product of the esterification reaction and the high polarity of the medium led to the leaching of the active phase of solid-supported catalysts and are challenging to overcome [67].

In this sense, Keggin HPAs Cs salts rise as an attractive option. Therefore, the activity of Keggin HPAs and their exchanged-partially cesium salts was evaluated in the esterification reactions of levulinic acid with alkyl alcohols. Levulinic esters are potential candidates for bioadditive of fuel or even as biofuel [37]. Previously, we have found that the homogenous acid  $\text{H}_4\text{SiW}_{12}\text{O}_{40}$  was an effective catalyst in levulinic acid esterification reactions at room

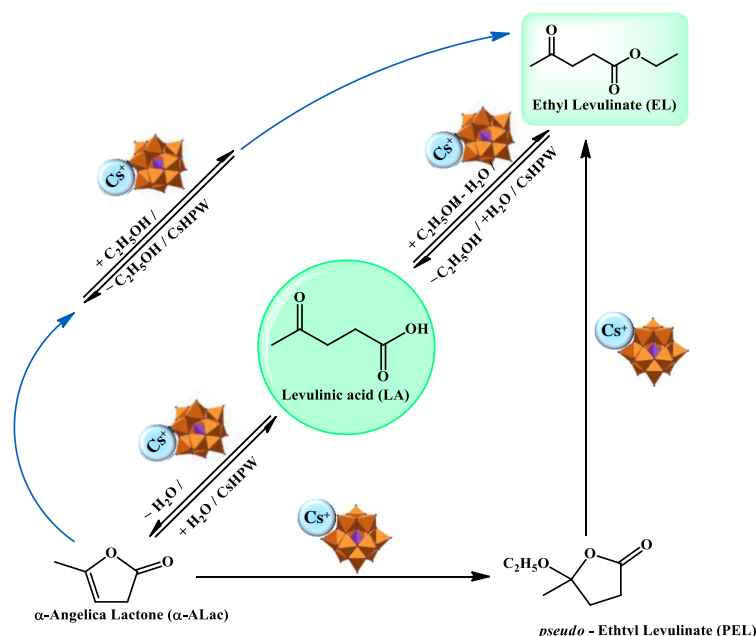
temperature [68]. However, herein as the catalyst remained solid in solution, a high reaction temperature was required.

Typically, catalytic runs were carried out in a sealed glass tube (25 mL), containing levulinic acid (2.0 mmol) dissolved in an alkyl alcohol solution (8 mL) under magnetic stirring, which was heated to 393 K in an oil bath. The addition of the acid catalyst (1.2 mol %) started the reaction [37].

Scheme 18 summarizes the main results achieved in the esterification reactions of levulinic acid with ethyl alcohol, in the presence of Keggin HPAs or their partially exchanged cesium salts. The selectivity toward ethyl levulinate, an ester with a carbon chain in the range of automotive liquid fuel is also highlighted.

The conversions and selectivity reached were higher for the reactions in the presence of tungsten catalysts (silico- or phosphotungstic). Although the highest conversion (i.e., 97%) has been attained on the  $H_3PW_{12}O_{40}$ -catalyzed reaction, it occurred in homogenous conditions. Therefore, the  $Cs_{2.5}H_{0.5}PW_{12}O_{40}$  catalyst was selected to study the effect of reaction variables [37].

In the presence of an acidic catalyst, the levulinic acid can be converted to ethyl levulinate following the reaction pathway shown in Scheme 19 as reported in the literature [52].



**Scheme 19.** Probable reaction pathways of conversion of levulinic acid to ethyl levulinate (adapted from ref. [37]).

Although the esterification type Fisher seems to be the most probable route, it is possible that depending on the strength of acidity of the catalyst, the levulinic acid suffers a lactonization process generating the angelic lactone or pseudo-ethyl levulinate, being then converted to ester.

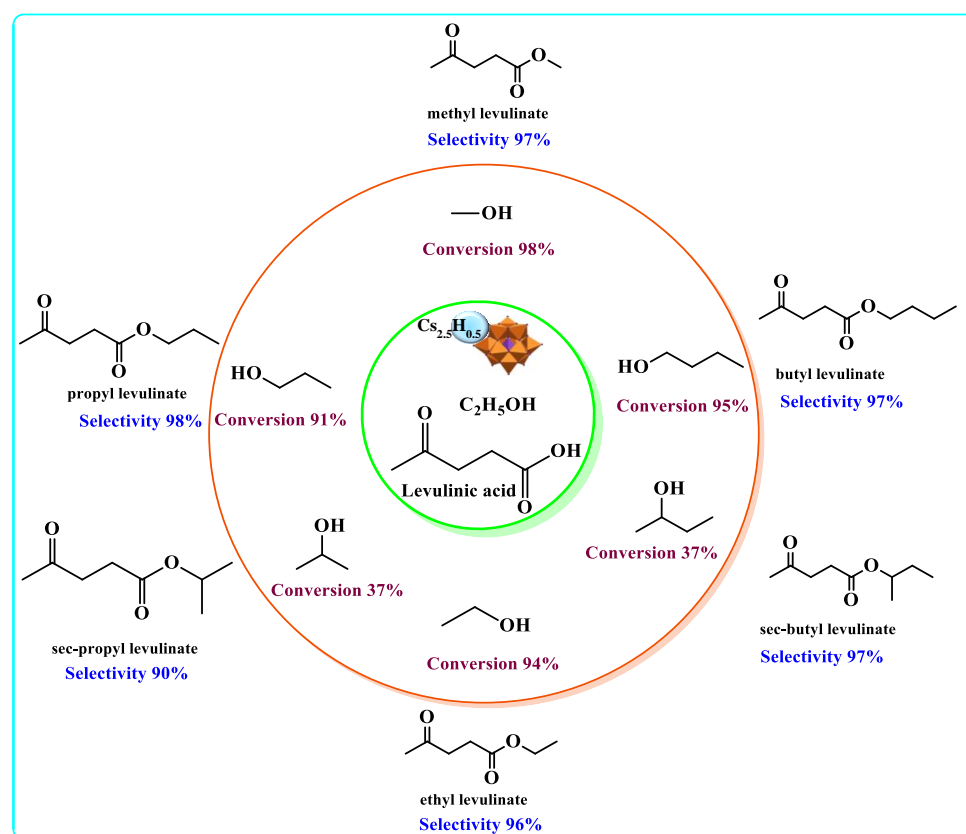
The impact of cesium load on the conversion and selectivity of levulinic acid esterification reactions with ethyl alcohol was investigated, the main results are shown in Table 1. The cesium load had a minimum impact on the conversion of Levulinic acid or ethyl levulinate selectivity. All of the cesium catalysts achieved conversions and selectivity equal to or greater than 90% (Table 1).

**Table 1.** Effects of cesium load on the conversion and selectivity of levulinic acid esterification reactions with ethyl alcohol in the presence of phosphotungstic acid or their exchanged-partially cesium salts (adapted from ref. [37])<sup>a</sup>.

Catalyst	Conversion of Levulinic Acid	Ethyl Levulinate Selectivity
H <sub>3</sub> PW <sub>12</sub> O <sub>40</sub>	97	97
Cs <sub>0.5</sub> H <sub>2.5</sub> PW <sub>12</sub> O <sub>40</sub>	96	96
CsH <sub>2</sub> PW <sub>12</sub> O <sub>40</sub>	96	95
Cs <sub>1.5</sub> H <sub>1.5</sub> PW <sub>12</sub> O <sub>40</sub>	95	94
Cs <sub>2</sub> HPW <sub>12</sub> O <sub>40</sub>	94	95
Cs <sub>2.5</sub> H <sub>0.5</sub> PW <sub>12</sub> O <sub>40</sub>	94	97
Cs <sub>3</sub> PW <sub>12</sub> O <sub>40</sub>	85	87

<sup>a</sup> Reaction conditions: levulinic acid (2 mmol), ethyl alcohol (8 mL), dodecane (internal standard), catalyst (1.2 mol%), temperature (393 K), time (6 h).

The Cs<sub>2.5</sub>H<sub>0.5</sub>PW<sub>12</sub>O<sub>40</sub>-catalyzed levulinic acid esterification reactions were also carried out with other alkyl alcohols (Scheme 20).



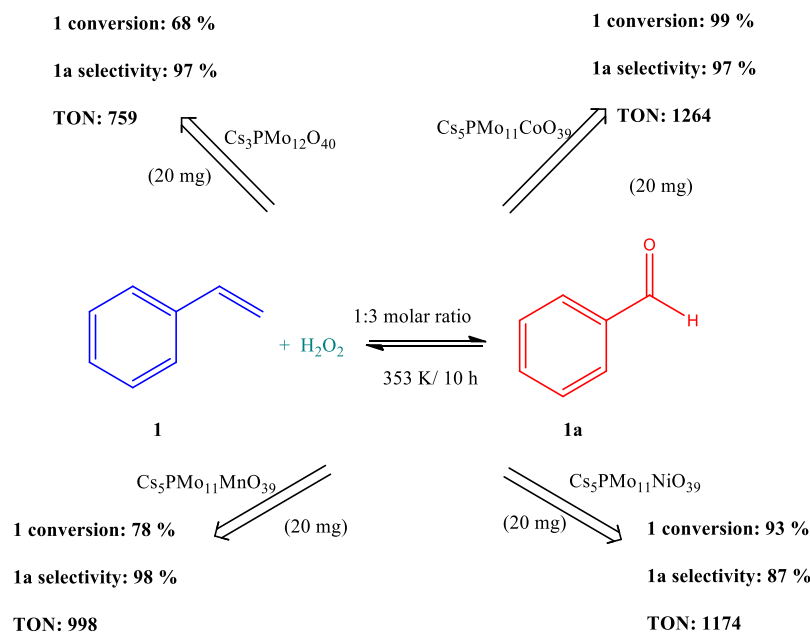
**Scheme 20.** Impacts of alcohol on the conversion and selectivity of Cs<sub>2.5</sub>H<sub>0.5</sub>PW<sub>12</sub>O<sub>40</sub>-catalyzed levulinic acid esterification reactions (adapted from ref. [37]).

An increase in the size of the alcohol carbon chain had a minimum impact on the conversion of levulinic acid esterification reactions. On the other hand, the conversions achieved in the reactions with secondary alcohols were significantly lower than primary ones. Conversely, regardless of the alcohol used, the selectivity toward alkyl levulinate was always equal to higher than 90% (Scheme 20) [37].

#### 4.2. Keggin HPA Cesium Salts as Catalysts in Oxidation Reactions

Patel and Patan reported the synthesis and detailed characterization of a Keggin-type cesium salt of transition metal-substituted phosphomolybdates, Cs<sub>5</sub>[PCo(H<sub>2</sub>O)-Mo<sub>11</sub>O<sub>39</sub>]·6H<sub>2</sub>O

and  $\text{Cs}_5[\text{PMn}(\text{H}_2\text{O})\text{Mo}_{11}\text{O}_{39}]\cdot 6\text{H}_2\text{O}$  [69]. Those authors evaluated the catalytic activity of cesium salts in oxidation reactions in the liquid phase of styrene using hydrogen peroxide as the oxidant. Cesium salts doped with Ni, Mn or Co were the catalysts assessed. Those authors assessed the catalytic activity of these salts, and the main results are in Scheme 21.



**Scheme 21.** Styrene oxidation with hydrogen peroxide over undoped and metal-doped cesium salts (adapted from ref. [69]).

The high TON, conversion and selectivity achieved in the reactions over these salts demonstrate that they are highly efficient heterogeneous catalysts. All of these salts were stable under reaction conditions and reused without loss of catalytic activity. Kinetic studies found the values of activation energy equal to 62, 76 and 67 kJ/mol for the reactions over  $\text{Cs}_5\text{PMo}_{11}\text{CoO}_{39}$ ,  $\text{Cs}_5\text{PMo}_{11}\text{MnO}_{39}$  and  $\text{Cs}_5\text{PMo}_{11}\text{NiO}_{39}$ , respectively [52]. The same authors used manganese-doped cesium phosphotungstate salt catalysts in oxidation reactions of styrene as different oxidants [70,71].

The kinetic curve in Figure 20 shows that this catalytic combination was less efficient than that using manganese-doped cesium phosphomolybdate salt and hydrogen peroxide [71].

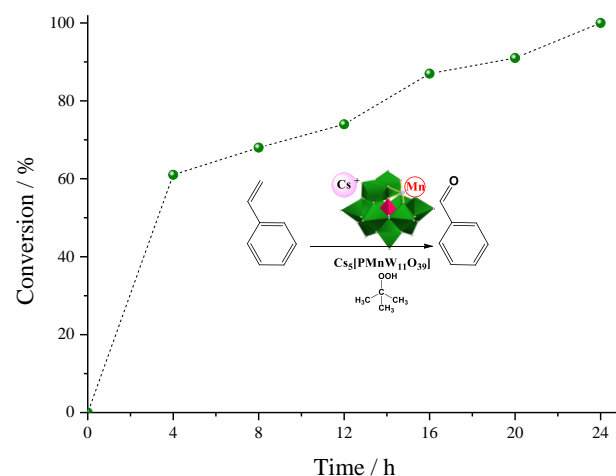
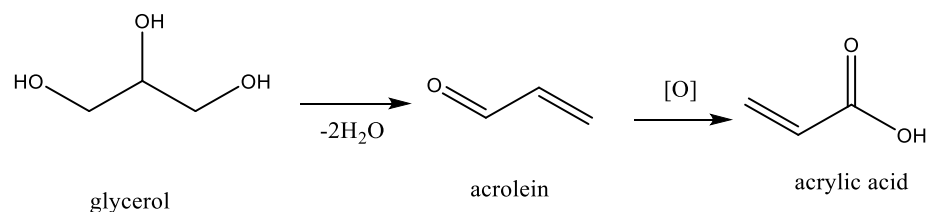


**Figure 20.**  $\text{Cs}_5\text{PW}_{11}\text{MnO}_{39}$ -catalyzed styrene oxidation (adapted from ref. [71]). Reaction conditions: Styrene (100 mmol), catalyst amount (25 mg), oxidant ( $\text{O}_2$ ), Co-oxidant-(TBHP; 2 mmol), temperature (353 K).

Another example of the use of cesium salts as catalysts in oxidative transformations was reported by Li and Zhang, which assesses the oxidative dehydration of glycerol to acrylic acid over vanadium-substituted cesium salts of Keggin HPAs [72]. Scheme 22 simply describes this reaction.



**Scheme 22.** Oxidative dehydration of glycerol to acrylic acid.

Figure 21 shows the results achieved in reactions carried out over vanadium-doped cesium phosphotungstate or phosphomolybdate. All the reactions were carried out using catalyst (0.2 g), temperature (613 K), carrier gas, 5% O<sub>2</sub>/He (20 mL min<sup>-1</sup>), feed (20 wt. % glycerol in H<sub>2</sub>O (0.5 mL h<sup>-1</sup>; WHSV: 0.5 h<sup>-1</sup>). 1 h time.

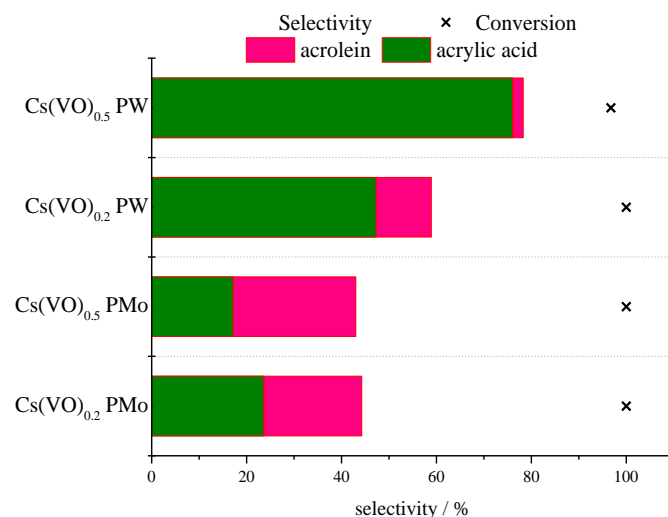


**Figure 21.** Oxidative dehydration of glycerol to acrylic acid over vanadium-doped cesium phosphotungstate or phosphomolybdate (adapted from ref. [72]).

The vanadium-doped cesium phosphomolybdate salts were more efficient catalysts than phosphotungstate, reaching higher conversions and selectivity to acrylic acid. Similarly, an increase in VO load had also a positive effect. It suggests that the strength of acidity of the catalyst plays a key role in these reactions.

Patan and Patel assessed the oxidation of alcohols in the presence of (Co, Mn, Ni)-substituted Keggin-phosphomolybdates catalysts using hydrogen peroxide [73]. Figure 22 shows that although the reactions in the presence of Cs<sub>5</sub>PMo<sub>11</sub>CoO<sub>39</sub> or Cs<sub>5</sub>PMo<sub>11</sub>NiO<sub>39</sub> salts have achieved the same conversions and TON, the Co-doped salt was less efficient to promote the oxidation of benzaldehyde to benzoic acid.

Table 2 summarizes the main reactions catalyzed by cesium heteropolyacid salts (i.e., acid-catalyzed, one-pot, hydrogenation, hydrolysis, esterification, acetylation, oxidation).



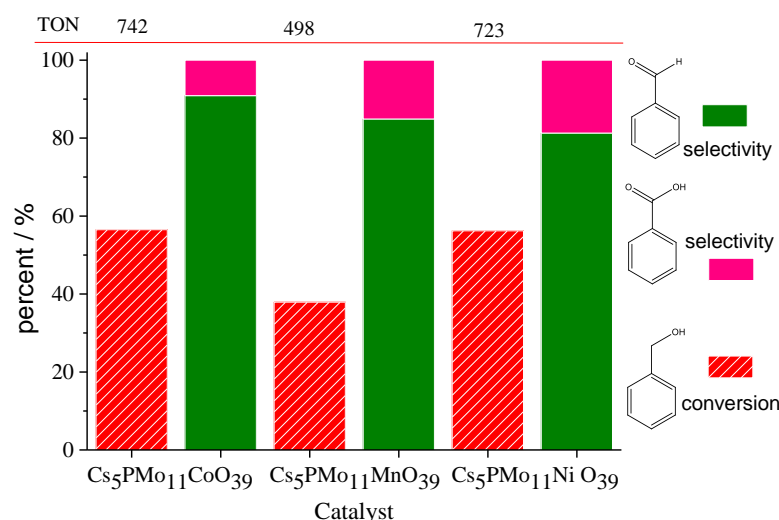


**Figure 22.** Benzyl alcohol oxidation with hydrogen peroxide over undoped and transition metal-doped cesium phosphomolybdate salts (adapted from ref. [73]).

**Table 2.** Application of Cs-salts HPAs in different catalytic processes.

Acidic Catalysis			
Reaction	Catalysts	Reference	
Furfural condensation reactions with alkyl alcohols	Cs <sub>2.5</sub> H <sub>0.5</sub> PW <sub>12</sub> O <sub>40</sub>	[35]	
β-pinene etherification with alkyl alcohols	Cs <sub>2.5</sub> H <sub>0.5</sub> PW <sub>12</sub> O <sub>40</sub>	[36]	
Levulinic acid esterification with alkyl alcohols	Cs <sub>2.5</sub> H <sub>0.5</sub> PW <sub>12</sub> O <sub>40</sub>	[37]	
Alkylation of toluene with benzyl alcohol	Cs <sub>3</sub> PMo <sub>12</sub> O <sub>40</sub>	[43]	
Hydrolysis of cellulose	Cs <sub>2.5</sub> H <sub>0.5</sub> PW <sub>12</sub> O <sub>40</sub>	[48]	
Glycerol esterification with acetic acid	Cs <sub>n</sub> H <sub>3-n</sub> PX <sub>12</sub> O <sub>40</sub> (n = 1.0–2.5) and Cs <sub>n</sub> H <sub>4-n</sub> SiY <sub>12</sub> O <sub>40</sub> , where X = W <sup>6+</sup> , Mo <sup>6+</sup> and Y = W <sup>6+</sup>	[54]	
Glycerol acetylation and esterification reactions with acetic anhydride and acetic acid	Cs <sub>2.5</sub> H <sub>0.5</sub> PW <sub>12</sub> O <sub>40</sub>	[74]	
Transesterification of glycerol tributyrate with methanol	Bimodal cesium hydrogen salts of 12-tungstosilicic acid Cs <sub>x</sub> H <sub>4-x</sub> SiW <sub>12</sub> O <sub>40</sub>	[75]	
Solvent-free self-condensation of levulinic acid	Cs <sub>x</sub> H <sub>4-x</sub> SiW <sub>12</sub> O <sub>40</sub>	[76]	
Hydrolysis of cellulose	Cs <sub>4-x</sub> H <sub>x</sub> SiW <sub>12</sub> O <sub>40</sub> (x = 3 and 3.5), Cs <sub>3-x</sub> H <sub>x</sub> PMo <sub>12</sub> O <sub>40</sub> and Cs <sub>3-x</sub> H <sub>x</sub> PW <sub>12</sub> O <sub>40</sub> (x = 2 and 2.5)	[77]	
Alkylation of toluene with benzyl alcohol	Nano Cs <sub>2.5</sub> H <sub>0.5</sub> PW <sub>12</sub> O <sub>40</sub>	[78]	
Prins cyclization of isoprenol and isovaleraldehyde to Florol®.	Cs <sub>2.5</sub> H <sub>0.5</sub> PW <sub>12</sub> O <sub>40</sub> /SiO <sub>2</sub> , Cs <sub>2.5</sub> H <sub>0.5</sub> PW <sub>12</sub> O <sub>40</sub>	[79]	
Oxidative reactions			
Styrene oxidation	Mn-doped cesium phosphomolybdate salts	[71]	
Alcohols oxidation with hydrogen peroxide	(Co, Mn, Ni)-substituted Keggin-phosphomolybdates	[73]	
Hydrogenation reactions			
Styrene hydrogenation	Cesium salt of iron substituted phosphomolybdate	[46]	
One-pot reactions			
Oxidative dehydration of glycerol to acrylic acid	vanadium-doped cesium phosphotungstate or phosphomolybdate	[72]	
Synthesis of one-pot two-component 1,3,4-oxadiazole derivatives	Cs <sub>3</sub> PW <sub>12</sub> O <sub>40</sub>	[80]	
One-pot synthesis of formic acid via hydrolysis–oxidation of potato starch	Cs <sub>3.5</sub> H <sub>0.5</sub> PW <sub>11</sub> VO <sub>40</sub> , Cs <sub>4.5</sub> H <sub>0.5</sub> SiW <sub>11</sub> VO <sub>40</sub> , Cs <sub>3.5</sub> H <sub>0.5</sub> PMo <sub>11</sub> VO <sub>40</sub> , Cs <sub>2.5</sub> H <sub>0.5</sub> PMo <sub>12</sub> O <sub>40</sub>	[81]	

## 5. Conclusions

The main methods of synthesis, characterization and catalytic applications of Keggin-type heteropolyacid cesium salts were discussed. A detailed description of the main routes to synthesize the various types of cesium heteropoly salts was performed, including saturated, lacunar, and metal-doped salts. Afterwards, the characterization of salts total or partially cesium exchanged was addressed, with emphasis on infrared spectroscopy, powder X-rays diffraction patterns, thermal analyses, surface area, volume and pores distribution, and measurements of strength and number of acid sites through potentiometric titration curves. Phosphotungstic, phosphomolybdic, and silicotungstic acids and their cesium salts were the goal catalysts. The use of these salts as heterogeneous catalysts in acid-catalyzed reactions (i.e., esterification, etherification, acetalization, dehydration) or oxidative transformations (oxidative esterification, oxidation) was addressed herein. This review discussed the most pertinent heterogeneous catalytic systems based on Keggin HPA Cs salts. The focus was to correlate the physicochemical properties of these salts with their catalytic activity. Cesium heteropoly salts are an alternative to the traditional soluble mineral acids as well as to solid-supported catalysts.

**Author Contributions:** Conceptualization, M.J.d.S.; methodology, M.J.d.S.; software, M.J.d.S., N.P.G.L. and A.A.R.; investigation, M.J.d.S., N.P.G.L. and A.A.R.; resources, M.J.d.S., N.P.G.L. and A.A.R.; writing—original draft preparation, M.J.d.S.; writing—review and editing, M.J.d.S.; supervision, M.J.d.S. All authors have read and agreed to the published version of the manuscript.

**Funding:** Coordenação de Aperfeiçoamento de Pessoal de Nível Superior—Brasil (CAPES—Finance Code 001).

**Data Availability Statement:** Not applicable.

**Acknowledgments:** The authors are grateful to the Brazilian research agencies, CAPES, FAPEMIG and CNPq for the financial support.

**Conflicts of Interest:** The authors declare no conflict of interest.

## References

1. Jambhulkar, D.K.; Ugwekar, R.P.; Bhanvase, B.A.; Barai, D.P. A review on solid base heterogeneous catalysts: Preparation, characterization, and applications. *Chem. Eng. Commun.* **2020**, *209*, 433–484. [[CrossRef](#)]
2. Helwani, Z.; Othman, M.R.; Aziz, N.; Fernando, W.J.N.; Kim, J. Technologies for production of biodiesel focusing on green catalytic techniques: A review. *Fuel Process. Technol.* **2009**, *90*, 1502–1514. [[CrossRef](#)]
3. Akinawo, C.A.; Mosia, L.; Alimi, O.A.; Oseghale, C.O.; Fapojuwo, D.P.; Bingwa, N.; Meijboom, R. Eco-friendly synthesis of valuable fuel bio-additives from glycerol. *Catal. Commun.* **2021**, *152*, 106287–106293. [[CrossRef](#)]
4. Nda-Umar, U.I.; Ramli, I.; Taufiq-Yap, Y.H.; Muhamad, E.N. An overview of recent research in the conversion of glycerol into biofuels, fuel additives and other biobased chemicals. *Catalysts* **2019**, *9*, 15. [[CrossRef](#)]
5. Lin, L.; Han, X.; Han, B.; Yang, S. Emerging heterogeneous catalysts for biomass conversion: Studies of the reaction mechanism. *Chem. Soc. Rev.* **2021**, *50*, 11270–11292. [[CrossRef](#)]
6. He, Q.; McNutt, J.; Yang, J. Utilization of the residual glycerol from biodiesel production for renewable energy generation. *Renew. Sustain. Energy Rev.* **2017**, *71*, 63–76. [[CrossRef](#)]
7. Nanda, M.R.; Yuan, Z.; Qin, W.; Ghaziaskar, H.R.; Poirer, M.A.; Xu, C.C. Thermodynamic and kinetic studies of a catalytic process to convert glycerol into solketal as an oxygenated fuel additive. *Fuel* **2014**, *117*, 470–477. [[CrossRef](#)]
8. Appaturi, J.N.; Ratti, R.; Phoon, B.L.; Batagarawa, S.M.; Din, I.U.; Selvaraj, M.; Ramalinga, R.J. A review of the recent progress on heterogeneous catalysts for Knoevenagel condensation. *Dalton Trans.* **2021**, *50*, 4445–4469. [[CrossRef](#)]
9. Ruiz, V.E.; Velty, A.; Santos, L.L.; Perez, L.A.; Sabater, M.J.; Iborra, S.; Corma, A. Gold catalysts and solid catalysts for biomass transformations: Valorization of glycerol and glycerol—Water mixtures through formation of cyclic acetals. *J. Catal.* **2010**, *271*, 351–357. [[CrossRef](#)]
10. Ballotin, F.C.; Da Silva, M.J.; Teixeira, A.P.C.; Lago, R.M. Amphiphilic acid carbon catalysts produced by bio-oil sulfonation for solvent-free glycerol ketalization. *Fuel* **2020**, *274*, 117779. [[CrossRef](#)]
11. Yang, X.F.; Wang, A.; Qiao, B.; Li, J.; Liu, J.; Zhang, T. Single-atom catalysts: A new frontier in heterogeneous catalysis. *Acc. Chem. Res.* **2013**, *46*, 1740–1748. [[CrossRef](#)] [[PubMed](#)]
12. Kozhevnikov, I.V. Heteropoly acids and related compounds as catalysts for fine chemical synthesis. *Catal. Rev.* **1995**, *37*, 311–352. [[CrossRef](#)]

13. Lai, S.Y.; Ng, K.H.; Cheng, C.K.; Nur, H.; Nurhadi, M.; Arumugam, M. Photocatalytic remediation of organic waste over Keggin-based polyoxometalate materials: A review. *Chemosphere* **2021**, *263*, 128244. [[CrossRef](#)] [[PubMed](#)]
14. Popa, A.; Sasca, V.; Kiš, E.E.; Radmila, J.; Marinkovi-Neducin, R.; Bokorov, M.T.; Halasz, M.T. Structure and texture of some Keggin type heteropolyacids supported on silica and titania. *J. Optoelectron. Adv. Mat.* **2005**, *7*, 3169–3177.
15. Ruiz, D.M.; Pasquale, G.A.; Martínez, J.J.; Romanelli, G.P. Advances in novel activation methods to perform green organic synthesis using recyclable heteropolyacid catalysis. *Green Process. Synth.* **2022**, *11*, 766–809. [[CrossRef](#)]
16. Amini, M.M.; Shaabani, A.; Bazgir, A. Tungstophosphoric acid ( $H_3PW_{12}O_{40}$ ): An efficient and eco-friendly catalyst for the one-pot synthesis of dihydropyrimidin-2(1H)-ones. *Catal. Commun.* **2006**, *7*, 843–847. [[CrossRef](#)]
17. Patil, M.R.; Yelamaggad, A.; Keri, R.S. A mild, efficient, and reusable solid phosphotungstic acid catalyst mediated synthesis of benzoxazole derivatives: A grinding approach. *Lett. Org. Chem.* **2016**, *13*, 474–481. [[CrossRef](#)]
18. Chaves, D.M.; Ferreira, S.O.; Chagas da Silva, R.; Natalino, R.; da Silva, M.J. Glycerol esterification over Sn(II)-exchanged Keggin heteropoly salt catalysts: Effect of thermal treatment temperature. *Energy Fuels* **2019**, *33*, 7705–7716. [[CrossRef](#)]
19. Umbarkar, S.B.; Kotbagi, T.V.; Biradar, A.V.; Pasricha, R.; Chanale, J.; Dongare, M.K.; Mamede, A.S.; Lancelot, C.; Payen, E.J. Acetalization of glycerol using mesoporous  $MoO_3/SiO_2$  solid acid catalyst. *Mol. Catal. A* **2009**, *310*, 150–158. [[CrossRef](#)]
20. Serafim, H.; Fonseca, I.M.; Ramos, A.M.; Vital, J.; Castanheiro, J.E. Valorization of glycerol into fuel additives over zeolites catalysts. *Chem. Eng. J.* **2011**, *178*, 291–296. [[CrossRef](#)]
21. Coronel, N.C.; Da Silva, M.J. Lacunar Keggin heteropolyacid salts: Soluble, solid, and solid-supported catalysts. *J. Clust. Sci.* **2018**, *29*, 195–205. [[CrossRef](#)]
22. Da Silva, M.J.; Teixeira, M.G.; Natalino, R. Highly selective synthesis under benign reaction conditions of furfural dialkyl acetal using  $SnCl_2$  as a recyclable catalyst. *New J. Chem.* **2019**, *43*, 8606–8612. [[CrossRef](#)]
23. Narkhede, N.; Patel, A. Sustainable valorisation of glycerol via acetalization as well as carboxylation reactions over silicotungstates anchored to zeolite H $\beta$ . *Appl. Catal. A* **2016**, *515*, 154–163. [[CrossRef](#)]
24. Srikanth, A.; Viswanadham, B.; Kumar, V.P.; Anipindi, N.R.; Chary, K.V.R. Synthesis and characterization of Cs-exchanged heteropolyacid catalysts functionalized with Sn for carbonolysis of glycerol to glycerol carbonate. *Appl. Petrochem. Res.* **2016**, *6*, 145–153. [[CrossRef](#)]
25. Ferreira, P.A.; Fonseca, I.M.; Ramos, A.M.; Vital, J.; Castanheiro, J.E. Valorization of glycerol by condensation with acetone over silica-included heteropolyacids. *Appl. Catal. B Environ.* **2010**, *98*, 94–99. [[CrossRef](#)]
26. Charson, N.; Amnuaypanich, S.; Soontaranon, S.; Rugmai, S.; Amnuaypanich, S. Increasing solketal production from the solventless ketalization of glycerol catalyzed by nanodispersed phosphotungstic acid in poly(N-methyl-4-vinylpyridinium) grafted on silica nanoparticles. *J. Indust. Eng. Chem.* **2022**, *112*, 233–243. [[CrossRef](#)]
27. Srinivas, M.; Raveendra, G.; Parameswaram, G.; Prasad, P.S.S.; Lingaiah, N. Cesium exchanged tungstophosphoric acid supported on tin oxide: An efficient solid acid catalyst for etherification of glycerol with *tert*-butanol to synthesize biofuel additives. *J. Mol. Catal. A* **2016**, *413*, 7–14. [[CrossRef](#)]
28. Narkhede, N.; Patel, A. Biodiesel production by esterification of oleic acid and transesterification of soybean oil using a new solid acid catalyst comprising 12-tungstosilicic acid and zeolite H $\beta$ . *Ind. Eng. Chem. Res.* **2013**, *52*, 13637–13644. [[CrossRef](#)]
29. Da Silva, M.J.; De Oliveira, C.M. Catalysis by Keggin Heteropolyacid Salts. *Curr. Catal.* **2018**, *7*, 26–34. [[CrossRef](#)]
30. Da Silva, M.J.; Liberto, N.A. Soluble and solid supported Keggin heteropolyacids as catalysts in reactions for biodiesel production: Challenges and recent advances. *Curr. Org. Chem.* **2016**, *20*, 1263–1283. [[CrossRef](#)]
31. Da Silva, M.J.; Ribeiro, C.J.A.; Vilanculo, C.B. How the content of protons and vanadium affects the activity of  $H_{3+n}PMO_{12-n}V_nO_{40}$  ( $n = 0, 1, 2, \text{ or } 3$ ) catalysts on the oxidative esterification of benzaldehyde with hydrogen peroxide. *Catal. Lett.* **2022**. [[CrossRef](#)]
32. Narkhede, N.; Patel, A. Efficient synthesis of biodiesel over a recyclable catalyst comprising a monolacunary silicotungstate and zeolite H $\beta$ . *RSC Adv.* **2014**, *4*, 64379–64387. [[CrossRef](#)]
33. Vilanculo, C.B.; Da Silva, M.J.; Rodrigues, A.A.; Ferreira, S.O.; Da Silva, R.C. Vanadium-doped sodium phosphomolybdate salts as catalysts in the terpene alcohols oxidation with hydrogen peroxide. *RSC Adv.* **2021**, *11*, 24072–24085. [[CrossRef](#)] [[PubMed](#)]
34. Da Silva, M.J.; Andrade, P.H.; Sampaio, V.F.C. Transition metal-substituted potassium silicotungstate salts as catalysts for oxidation of terpene alcohols with hydrogen peroxide. *Catal. Lett.* **2021**, *151*, 2094–2106. [[CrossRef](#)]
35. Da Silva, M.J.; Lopes, N.P.G.; Bruziquesi, C.G.O. Furfural acetalization over Keggin heteropolyacid salts at room temperature: Effect of cesium doping. *React. Kinet. Mech. Catal.* **2021**, *133*, 913–931. [[CrossRef](#)]
36. Da Silva, M.J.; Lopes, N.P.G.; Ferreira, S.O.; Da Silva, R.C.; Natalino, R.; Chaves, D.M.; Teixeira, M.G. Monoterpenes etherification reactions with alkyl alcohols over cesium partially exchanged Keggin heteropoly salts: Effects of catalyst composition. *Chem. Pap.* **2021**, *75*, 153–168. [[CrossRef](#)]
37. Lopes, N.P.G.; Da Silva, M.J. Cesium partially exchanged heteropolyacid salts: Efficient solid catalysts to produce bioadditives from the levulinic acid esterification with alkyl alcohols. *React. Kinet. Mech. Catal.* **2022**, *135*, 3173–3184. [[CrossRef](#)]
38. Pizzio, L.R.; Blanco, M.N. A contribution to the physicochemical characterization of nonstoichiometric salts of tungstosilicic acid. *Microporous Mesopor. Mater.* **2007**, *103*, 40–47. [[CrossRef](#)]
39. Park, H.W.; Park, S.; Park, D.R.; Choi, J.H.; Song, I.K. Decomposition of phenethyl phenyl ether to aromatics over  $Cs_xH_{3.0-x}PW_{12}O_{40}$  ( $X = 2.0\text{--}3.0$ ) heteropolyacid catalysts. *Catal. Commun.* **2010**, *12*, 35. [[CrossRef](#)]
40. Dias, J.A.; Caliman, E.; Dias, S.C.L. Effects of cesium ion exchange on the acidity of 12-tungstophosphoric acid. *Micropor Mesopor. Mater.* **2004**, *76*, 221–232. [[CrossRef](#)]

41. Chai, F.; Cao, F.; Zhai, F.; Chen, Y.; Wang, X.; Su, Z. Transesterification of vegetable oil to biodiesel using a heteropolyacid solid catalyst. *Adv. Synth. Catal.* **2007**, *349*, 1057–1065. [CrossRef]
42. Molchanov, V.V.; Maksimov, G.M.; Gojdin, V.V.; Kulikov, S.M.; Kulikova, O.M.; Kozhevnikov, I.V.; Bujanov, R.A.; Maksimovskaja, R.I.; Pljasova, L.M.; Lapina, O.B. Method of Preparing Phosphorus Heteropolyacids. RU 2076070 C1. 1997. Available online: <https://www.elibrary.ru/item.asp?id=38057690> (accessed on 1 January 2023).
43. Gu, Q.; Shi, S.; Liu, X.; Lian, H.; Wang, T.; Heng Zhang, H. Effects of preparation method on the catalytic properties and deactivation behaviors of acidic cesium phosphomolybdate for the alkylation of toluene with benzyl alcohol. *React. Kinet. Mech. Catal.* **2022**, *135*, 1819–1834. [CrossRef]
44. Batalha, D.C.; Ferreira, S.O.; Da Silva, R.C.; Da Silva, M.J. Cesium-Exchanged Lacunar Keggin Heteropolyacid Salts: Efficient Solid Catalysts for the Green Oxidation of Terpenic Alcohols with Hydrogen Peroxide. *Chem. Select* **2020**, *5*, 1976–1986. [CrossRef]
45. Da Silva, M.J.; Andrade, P.H.S.; Ferreira, S.O.; Vilanculo, C.B.; Oliveira, C.M. Monolacunary K8SiW11O39-catalyzed terpenic alcohols oxidation with hydrogen peroxide. *Catal. Lett.* **2018**, *148*, 2516–2527. [CrossRef]
46. Patel, A.U.; Patel, J.R. Cesium salt of iron substituted phosphomolybdate: Synthesis, characterization, room temperature hydrogenation of styrene and its mechanistic evaluation. *Mol. Catal.* **2021**, *513*, 111827–111837. [CrossRef]
47. Hiyoshi, N.; Kamiya, Y. Observation of microporous cesium salts of 12-tungstosilicic acid using scanning transmission electron microscopy. *Chem. Commun.* **2015**, *51*, 9975–9978. [CrossRef]
48. Okuhara, T. Water-Tolerant Solid Acid Catalysts. *Chem. Rev.* **2002**, *102*, 3641–3666. [CrossRef]
49. Drago, R.S.; Dias, J.A.; Maier, T.O. An Acidity Scale for Brønsted Acids Including H<sub>3</sub>PW<sub>12</sub>O<sub>40</sub>. *J. Am. Chem. Soc.* **1997**, *119*, 7702. [CrossRef]
50. Deng, W.; Zhang, Q.; Wang, Y. Polyoxometalates as efficient catalysts for transformations of cellulose into platform chemicals. *Dalton Trans.* **2012**, *41*, 9817–9831. [CrossRef] [PubMed]
51. Pathan, S.; Patel, A. Keggin type transition metal substituted phosphomolybdates: Heterogeneous catalysts for selective aerobic oxidation of alcohols and alkenes under solvent-free condition. *Catal. Sci. Technol.* **2014**, *4*, 648–656. [CrossRef]
52. Karinen, R.S.; Krause, A.O.I. New Biocomponents from Glycerol. *Appl Catal A* **2006**, *306*, 128–133. [CrossRef]
53. Subhash, M.; Pal, D.B.; Jana, S.K. Biofuels Additives Derived via Clay Supported Heteropoly Acid Catalyzed Etherification of Glycerol with *tert*-Butanol-Biomass to Liquid Oxygenates. *Chem. Pap.* **2022**, *76*, 775–784. [CrossRef]
54. Veluturia, S.; Narula, A.; Shetty, S.P. Kinetic study of synthesis of bio-fuel additives from glycerol using a heteropolyacid. *Resour. Technol.* **2017**, *3*, 337–341. [CrossRef]
55. Tsolakis, N.; Bam, W.; Srai, J.S.; Kumar, M. Renewable chemical feedstock supply network design: The case of terpenes. *J. Clean Prod.* **2019**, *222*, 802–822. [CrossRef]
56. Corma, A.; Iborra, S.; Velty, A. Chemical Routes for the Transformation of Biomass into Chemicals. *Chem. Rev.* **2007**, *107*, 2411–2502. [CrossRef]
57. Masyita, A.; Sari, R.M.; Astuti, A.D.; Yasir, B.; Rumata, N.R.; Emran, T.B.; Nainu, F.; Simal-Gandara, J. Terpenes and terpenoids as main bioactive compounds of essential oils, Terpenes and terpenoids as main bioactive compounds of essential oils, their roles in human health and potential application as natural, food preservatives. *Food Chem. X* **2022**, *13*, 100217–100231. [CrossRef]
58. Montané, D.; Salvadó, J.; Torras, C.; Farriol, X. High-Temperature Dilute-Acid Hydrolysis of Olive Stones for Furfural Production. *Biomass Bioenerg.* **2002**, *22*, 295–304. [CrossRef]
59. Zeitsch, K.J. *The Chemistry and Technology of Furfural and Its Many By-Products*, 1st ed.; Elsevier: Amsterdam, The Netherlands, 2000.
60. Monteiro, J.L.F.; Veloso, C.O. Catalytic conversion of terpenes into fine chemicals. *Top. Catal.* **2004**, *27*, 169–180. [CrossRef]
61. Bozell, J.J.; Petersen, G.R. Technology development for the production of biobased products from biorefinery carbohydrates—the US Department of Energy’s “Top 10” revisited. *Green Chem.* **2010**, *12*, 539–554. [CrossRef]
62. Mascal, M.; Nikitin, E.B. High-yield conversion of plant biomass into the key value-added feedstocks 5- (hydroxymethyl)furfural, levulinic acid, and levulinate esters via 5-(chloromethyl)furfural. *Green Chem.* **2010**, *12*, 370–373. [CrossRef]
63. Gurbuz, E.I.; Alonso, D.M.; Bond, J.Q.; Dumesic, J.A. Reactive extraction of levulinate esters and conversion to  $\gamma$ -valerolactone for production of liquid fuels. *ChemSusChem* **2011**, *4*, 357–361. [CrossRef] [PubMed]
64. Xu, G.-Z.; Chang, C.; Zhu, W.-N.; Li, B.; Ma, X.-J.; Du, F.-G. A comparative study on direct production of ethyl levulinate from glucose in ethanol media catalysed by different acid catalysts. *Chem. Pap.* **2013**, *67*, 1355–1363. [CrossRef]
65. Joshi, H.; Moser, B.R.; Toler, J.; Smith, W.F.; Walker, T. Ethyl levulinate: A potential bio-based diluent for biodiesel which improves cold flow properties. *Biomass Bioenerg.* **2011**, *35*, 3262–3266. [CrossRef]
66. Saravanamurugan, S.; Riisager, A. Solid acid catalysed the formation of ethyl levulinate and ethyl glucopyranoside from mono- and disaccharides. *Catal. Commun.* **2012**, *17*, 71–75. [CrossRef]
67. Fernandes, D.R.; Rocha, A.S.; Mai, E.F.; Mota, C.J.A.; Teixeira da Silva, V. Levulinic acid esterification with ethanol to ethyl levulinate production over solid acid catalysts. *Appl. Catal. A* **2012**, *425–426*, 199–204. [CrossRef]
68. Vilanculo, C.B.; de Andrade Leles, L.C.; Da Silva, M.J. H<sub>4</sub>SiW<sub>12</sub>O<sub>40</sub>-Catalyzed Levulinic Acid Esterification at Room Temperature for Production of Fuel Bioadditives. *Waste Biomass Valor* **2020**, *11*, 1895–1904. [CrossRef]
69. Patel, A.; Pathan, S. Keggin-type cesium salt of first series transition metal-substituted phosphomolybdates: One-pot easy synthesis, structural, and spectral analysis. *J. Coord. Chem.* **2012**, *65*, 3122–3132. [CrossRef]
70. Pathan, S.; Patel, A. Transition-Metal-Substituted Phosphomolybdates: Catalytic and Kinetic Study for Liquid-Phase Oxidation of Styrene. *Ind. Eng. Chem. Res.* **2013**, *52*, 11913–11919. [CrossRef]

71. Patel, K.; Shringarpure, P.; Patel, A. One-step synthesis of a Keggin-type manganese(II)-substituted phosphotungstate: Structural and spectroscopic characterization and non-solvent liquid phase oxidation of styrene. *Transit. Met. Chem.* **2011**, *36*, 171–177. [[CrossRef](#)]
72. Li, X.; Zhang, Y. Oxidative Dehydration of Glycerol to Acrylic Acid over Vanadium-Substituted Cesium Salts of Keggin-Type Heteropolyacid. *ACS Catal.* **2016**, *6*, 2785–2791. [[CrossRef](#)]
73. Pathan, S.; Patel, A. Solvent-free clean selective oxidation of alcohols catalyzed by mono transition metal (Co, Mn, Ni)-substituted Keggin-phosphomolybdates using hydrogen peroxide. *Appl. Catal. A* **2013**, *459*, 59–64. [[CrossRef](#)]
74. Sandesh, S.; Manjunathan, P.; Halgeri, A.B.; Shanbha, G.V. Glycerol acetins: Fuel additive synthesis by acetylation and esterification of glycerol using cesium phosphotungstate catalyst. *RSC Adv.* **2015**, *5*, 104354–104362. [[CrossRef](#)]
75. Iwase, Y.; Sano, S.; Mahardiani, L.; Abe, R.; Kamiy, Y. Bimodal cesium hydrogen salts of 12-tungstosilicic acid,  $Cs_xH_{4-x}SiW_{12}O_{40}$ , as highly active solid acid catalysts for transesterification of glycerol tributyrate with methanol. *J. Catal.* **2014**, *318*, 34–42. [[CrossRef](#)]
76. Xi, X.; Sun, D.; An, H.; Wang, Y. Cesium silicotungstate catalyzed solvent-free self-condensation of levulinic acid and its product identification. *Biomass Conv. Bioref.* **2022**. [[CrossRef](#)]
77. Gromov, N.V.; Medvedeva, T.B.; Taran, O.P.; Timofeeva, M.N.; Parmon, V.N. Hydrolysis of Cellulose in the Presence of Catalysts Based on Cesium Salts of Heteropoly Acids. *Catal. Ind.* **2021**, *13*, 73–80. [[CrossRef](#)]
78. Akbay, E.; Demir, G. Nano-12-Tungstophosphoric Acid Cesium Salt Synthesized by Ultrasound as Catalyst for Alkylation of Benzene with dec-1-ene. *Int. J. Chem. React. Eng.* **2017**, *15*, 20160189. [[CrossRef](#)]
79. de Meireles, A.L.P.; Kelly, A.; da Silva Rocha, K.A.; Kozhevnikova, E.F.; Kozhevnikov, I.V.; EGusevskaya, E.V. Heteropoly acid catalysts in Prins cyclization for the synthesis of Florol<sup>®</sup>. *Mol. Catal.* **2021**, *502*, 111382. [[CrossRef](#)]
80. Alotaibi, M.A.; Bakht, M.A.; Alharthi, A.I.; Geesi, M.; Alshammar, M.B.; Riadi, Y. Facile preparation of cesium salt of tungstophosphoric acid for catalytic synthesis of one-pot two-component 1,3,4-oxadiazole derivatives in water: A doubly green approach. *Sustain. Chem. Pharm.* **2020**, *17*, 100279–100288. [[CrossRef](#)]
81. Gromov, N.V.; Medvedeva, T.B.; Rodikova, Y.A.; Babushkin, D.E.; Panchenko, V.N.; Timofeeva, M.N.; Zhizhina, E.G.; Taran, O.P.; Parmon, V.N. One-pot synthesis of formic acid via hydrolysis–oxidation of potato starch in the presence of cesium salts of heteropoly acid catalysts. *RSC Adv.* **2020**, *10*, 28856–28864. [[CrossRef](#)]

**Disclaimer/Publisher’s Note:** The statements, opinions and data contained in all publications are solely those of the individual author(s) and contributor(s) and not of MDPI and/or the editor(s). MDPI and/or the editor(s) disclaim responsibility for any injury to people or property resulting from any ideas, methods, instructions or products referred to in the content.